Mechanics of plio-quaternary faulting around the Karliova triple junction: implications for the deformation of Eastern part of the Anatolian *Scholle*

Taylan Sançar, H. Serdar Akyüz, Guido Schreurs & Cengiz Zabcı

View supplementary material 🗗

Published online: 14 Oct 2018.

Submit your article to this journal 🗗

Article views: 229

View Crossmark data 🗗

Taylor & Francis
Taylor & Francis Group

ARTICLE

Mechanics of plio-quaternary faulting around the Karliova triple junction: implications for the deformation of Eastern part of the Anatolian *Scholle*

Taylan Sançar[a,b], H. Serdar Akyüz [c], Guido Schreurs[d] and Cengiz Zabcı[c]

[a]Mühendislik Fakültesi, Jeoloji Mühendisliği Bölümü, Munzur Üniversitesi, Aktuluk, Tunceli, Turkey; [b]Ayazağa Yerleşkesi, Avrasya Yer Bilimleri Enstitüsü, İstanbul Teknik Üniversitesi, Maslak, İstanbul, Turkey; [c]Ayazağa Yerleşkesi, Maden Fakültesi, Jeoloji Mühendisliği Bölümü, İstanbul Teknik Üniversitesi, Maslak, İstanbul, Turkey; [d]Institut für Geologie, Universität Bern, Bern, Schweiz

ABSTRACT

The intersection of the Eurasian and Arabian plates and the smaller Anatolian Scholle created the Karlıova Triple Junction (KTJ) in eastern Turkey. In this study, we present analogue model experiments for this region and compare the results with our field observations and data from remote sensing imagery. Our comparison suggests that the sense of slip along curvilinear faults at the west of the KTJ changes along strike moving away from the principal displacement zones, from strike-slip to oblique normal and then to pure normal slip. Although, the active Prandtl cell model has been proposed to explain the overall regional fault pattern at eastern part of the Anatolian Scholle, the map view orientation of the secondary faults within the Karlıova wedge and performed analogue modelling results suggest that the passive wedge-shaped Prandtl cell model with a normal dip-slip component along slip lines is more appropriate in order to explain not only deformation pattern around the KTJ but also internal deformation of eastern part of the Anatolia. Moreover, these faults accumulate the significant amount of deformation that causes to the irregular earthquake behavior and the relatively lower geologic slip-rates along the main fault branch of boundary faults around the KTJ.

Abbreviations: Strike-slip; Karlıova Triple Junction (KTJ); continental deformation; North Anatolian Fault Zone (NAFZ); East Anatolian Fault Zone (EAFZ);Varto Fault Zone (VFZ)

1. Introduction

The basic assumption of plate tectonics is that the plates are rigid and that deformation between two lithospheric plates is confined to a narrow zone along its mutual boundary (Le Pichon, 1968; McKenzie & Parker, 1967; Morgan, 1968; Wilson, 1965). The situation is more complex when three lithospheric plates meet at a triple junction (Cronin, 1992; McKenzie & Morgan, 1969). Deformation at the triple junction depends on the nature of the plate boundaries and is mostly governed by the physical properties of the crust and upper mantle of the three plates involved and by the finite volume related to the temporal behavior of sea-floor spreading centers and subduction zones (Şengör, 2014). Observations worldwide, however, indicate that deformation at some plate boundaries is not confined to narrow deformation zones, but occurs over diffuse zones that cover about 15% of the earth's surface (Gordon, 1998). Hence, the meeting of three plates with at least one or all having such a diffuse boundary may result in a diffuse triple junction (Marques, Cobbold, & Lourenço, 2007; Royer & Gordon, 1997) show different behaviors in the oceanic and in the continental lithosphere

(Şengör, 2014). When the tectonic setting only involves continental lithosphere, compatibility problems may create geologically complex regions at or near the triple junction (Şengör, Görür, & Şaroğlu, 1985).
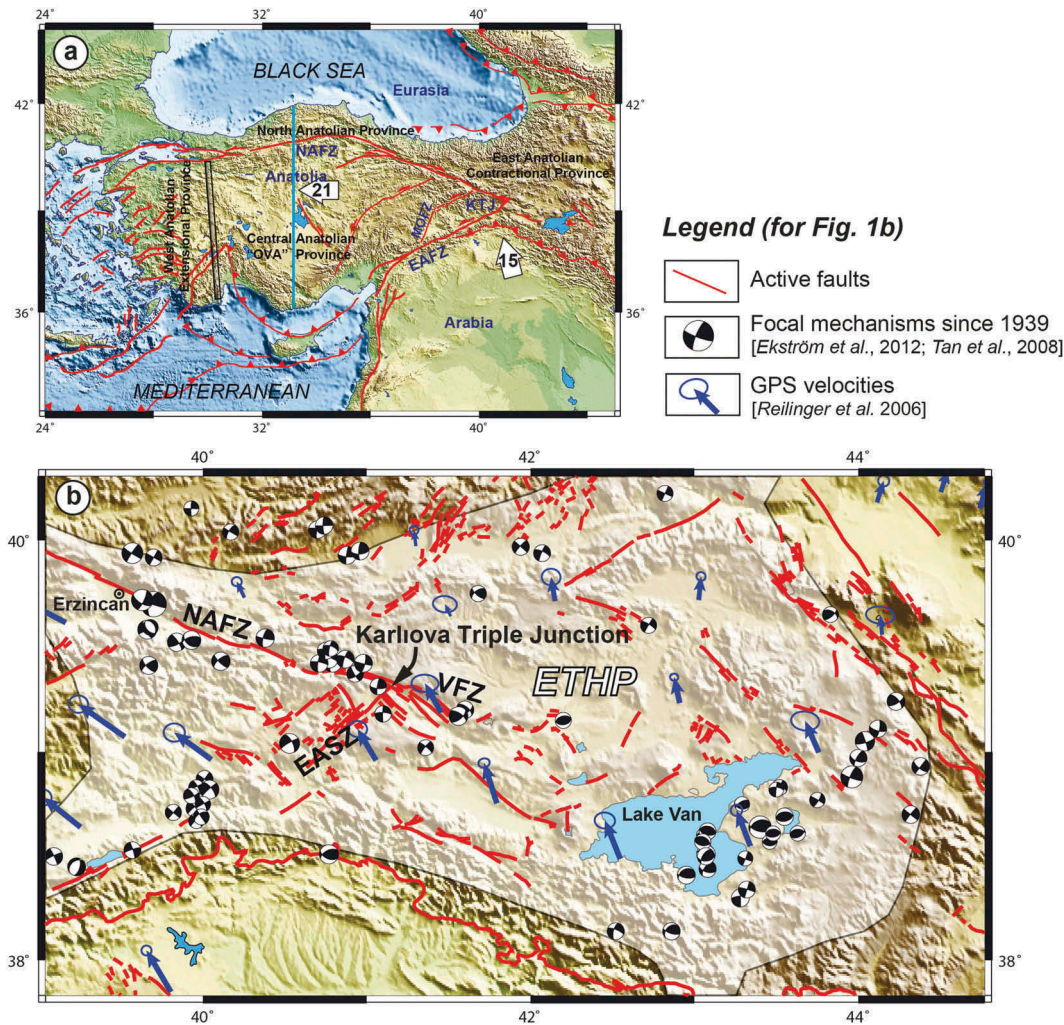
The Karlıova Triple Junction (KTJ) in eastern Turkey is such an ideal point in a continental crust, where the Eurasian and Arabian plates and the Anatolia meet (Figure 1) (Şengör, 2014; Şengör et al., 1985). Since the deformational pattern of Anatolia is characterized by the interaction of crustal fragments bounded by different fault belts (normal, reverse and strike-slip), it has been proposed that *Scholle* is a more appropriate term to define the tectonic behavior and nature of Anatolia than 'plate' (Dewey and Şengör, 1979). The Anatolian *Scholle*, which represents one of the most outstanding intraplate regions in the eastern Mediterranean region, is bounded by two large strike-slip fault zones, the North Anatolian Fault Zone (NAFZ) and the East Anatolian Fault Zone (EAFZ), marking the northern and southeastern boundaries (Şengör, 1980; Şengör et al., 1985), respectively (Figure 1(a)). The boundary between

Figure 1. (a) The simplified major tectonics structures in Turkey and the surrounding region (Akyuz, Altunel, Karabacak, & Yalciner, 2006; Avagyan et al., 2010; Duman & Emre, 2013; Hall, Aksu, Elitez, Yaltırak, & Çifçi, 2014; Koçyiğit & Beyhan, 1998; Le Pichon, Chamot-Rooke, L., Noomen, & Veis, 1995; Nyst & Thatcher, 2004; Philip, Cisternas, Gvishiani, & Gorshkov, 1989; Şaroğlu, Emre, & Kuşçu, 1992; Searle, Chung, & Lo, 2010; Şengör et al., 1985, 2014, 2005; Shaw & Jackson, 2010) All red lines with saw teeth indicates compression; lines with hachures represent normal faults; and all solid lines are strike-slip faults with red arrow indicating sense of relative displacement. Key to lettering: NAFZ – North Anatolian Fault Zone, EAFZ – East Anatolian Fault Zone, MOF – Malatya–Ovacık Fault. Base map is from GEBCO database (http://www.gebco.net/data_and_products/gridded_bathyme try_data/). (b) Map showing the eastern North Anatolian Fault Zone, the northern East Anatolian Fault Zone and the Eastern Turkish High Plateau (ETHP – the white shaded region) and surrounding active fault structures (Şaroğlu, Emre, & Kuşçu, 1992). Focal mechanisms are compiled from the Harvard Centroid Moment Tensor (CMT) database. Global Positioning System (GPS) vectors were plotted using the data of (Reilinger et al., 2006). The base map is the hillshade relief made from the Shuttle Radar Topographic Mission SRTM) v4 dataset (Jarvis, Reuter, Nelson, & Guevara, 2008).

the Eurasian and Arabian plate is distributed in a wide zone, mostly represented by discrete structures of a long-lived transpressional setting, named the Varto Fault Zone (VFZ) (Figure 2) (Sançar, Zabcı, Akyüz, Sunal, & Villa, 2015). The discussions on the stationary (Sançar et al., 2015; Şengör, 1979, 2014; Şengör et al., 1985; Zabcı, Sançar, Akyüz, & Kıyak, 2015a) or migrating (Barka & Gülen, 1988; Hubert-Ferrari et al., 2009; Westaway & Arger, 2001; Westaway, Demir, & Seyrek, 2008) nature of the continental KTJ and the surrounding structural complexity make this region of particular interest. Although recent publications discuss the faulting around the VFZ in details, to the east of the KTJ, (Gürboğa, 2016; Hubert-Ferrari et al., 2009;

Karaoğlu, Selçuk, & Gudmundsson, 2017; Sançar et al., 2015) and propose different faulting mechanisms, they provide less information on the distribution of faults and their mechanics for the region west of around the KTJ (Gürboğa, 2016; Hubert-Ferrari, Armijo, King, Meyer, & Barka, 2002; Karaoğlu et al., 2017; Tutkun & Hancock, 1990).

The NAFZ and EAFZ together have a V-shaped geometry in map view. Such a configuration of continental strike-slip faults is observed in various parts of the Earth (e.g. Taylor & Yin, 2009; Yin, 2010; Yin & Taylor, 2011) and has been the subject of numerous studies: (a) focusing on the deformation characteristics of the region between bounding faults (Cummings, 1976; Ingles, Dauch, Soula, Viallard, & Brusset, 1999) using
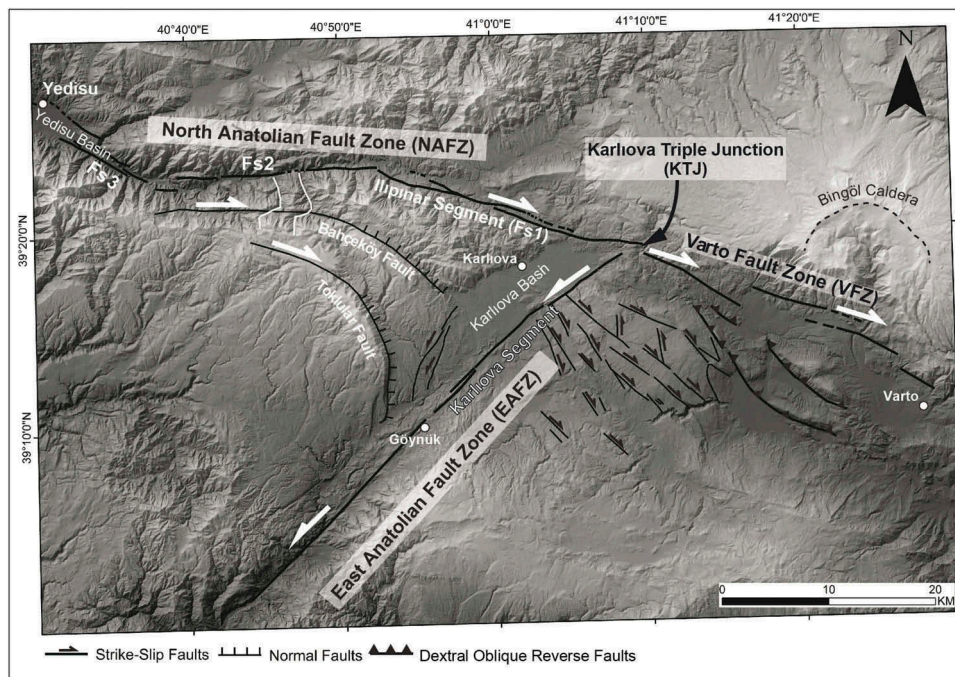
Figure 2. Active faults around the Karlıova Triple Junction. The base map is the hillshade of 10 m-ground pixel resolution digital elevation model produced from interpolation of 1:25000 scale elevation contours. Fs = Fault segment; white deflected lines = offset rivers.

modified versions of the original Prandtl cell model (Prandtl, 1924), (b) discussing the role of V-shaped faults in the context of lateral escape of the continental lithosphere (Ratschbacher, Merle, Davy, & Cobbold, 1991; Şengör, 1979; Tapponnier, Peltzer, & Armijo, 1986), and (c) dealing with the mechanical origin of V-shaped conjugate strike-slip fault systems (Yin & Taylor, 2011).

By comparing the geometry of V-shaped plate-boundary, other intraplate faults of the Anatolian *Scholle* (between the blue vertical line and KTJ in Figure 1) and the slip lines of the Prandtl Cell Model (Kanizay, 1962; Nadai, 1950), Şengör (1979) and Şengör et al. (1985) suggest the active Prandtl cell model is appropriate to explain the origin of internal deformation within the Anatolia. However, geometry and sense of slip lines of passive Prandtl cell model resemble the surface fault geometry that formed between the NAFZ and EAFZ in the Karlıova region at the easternmost part of the Anatolian *Scholle* (Figure 2). Therefore, understanding of how the curvilinear faults formed near west of the KTJ will contribute to better understanding of deformation processes at the easternmost part of the Anatolian *Scholle*

In this study, we discuss the structures in the vicinity of the KTJ (referred to here as the Karlıova region), particularly west of it where the complex deformation is the result of the interaction of the NAFZ and EAFZ. We first present an overview of the geology of the Karlıova region, which is followed by the description of the structures in this region that defined by using satellite images, aerial stereographic

aerial photographs, digital elevation models and field observations. Then, we compare the mapped structures with the results of passive Prandtl cell model based analogue model experiments, which provide a more reasonable causal relationship between the NAFZ, the EAFZ and the tectonic structures between them. These results present valuable data for understanding not only the evolution of the Plio-Quaternary tectonics structures around KTJ but also active faulting within the eastern part of the Anatolian *Scholle*.

2. Active tectonics and geology of the karliova triple junction (ktj)

2.1. Tectonic framework

Northward convergence of the Arabian and African plates with respect to Eurasian plate control the active deformation in the eastern Mediterranean region (Le Pichon & Kreemer, 2010; McKenzie, 1972; Şengör et al., 1985) (Figure 1(a)). In this complex tectonic setting, the westward extrusion of Anatolia in mainly controlled by; (a) the convergence between Arabia and Eurasia and extra forces from beneath or force from the gravitational potential of the East Anatolia High Plateau (McKenzie, 1972; Özeren and Holt, 2010; Şengör et al., 1985), (b) slab pull of the Hellenic subduction (Reilinger et al., 2006), (c) asthenospheric flow dragging the circular motion of lithosphere from the Levant in the east to Anatolia and Aegean in the west (Le Pichon & Kreemer, 2010), or (d) combination of the effect of slab pull with a mantle upwelling underneath Afar

and with the large-scale flow associated with a whole mantle, Tethyan convection cell (Faccenna et al., 2013). It is generally accepted that almost all of the present-day deformation accumulate along the NAFZ and EAFZ (Kozacı, Dolan, & Finkel, 2009; Reilinger et al., 2006; Şengör, 1980; Şengör et al., 1985, 2005). However, recent studies show the significant amount of deformation within the internal parts of Anatolia, where bulk strain cause to formation of new structures and reactivation of early structures (Bozkurt, 2001), during its westward motion (Aktuğ, Dikmen, Dogru, & Ozener, 2013a; Aktuğ et al., 2013b; Higgins et al., 2015; Özener et al., 2010; Sarıkaya, Yıldırım, & Çiner, 2015; Yazıcı, Zabcı, Sançar, & Natalin, 2018b; Yazıcı, Zabcı, Sançar, Sunal, & Natalin, 2016; Yıldırım, 2014; Yıldırım, Sarıkaya, & Çiner, 2016).

The NW-striking dextral and NE-striking sinistral strike-slip faults (between the blue vertical line and KTJ in Figure 1) are the prominent tectonic structures that participate the intraplate deformation of the Anatolia. The ongoing debates, which have a strong relationship with the behavior of the KTJ, about these faults are (a) how they formed and (b) whether they are active or not?

The pioneering hypothesis asserts that the NW-striking dextral and NE-striking sinistral strike-slip faults (between the blue vertical line and KTJ in Figure 1) are clearly fit to active Prandtl cell model of the Varnes (1962) and the KTJ is holding *in situ* (Şengör, 1980; Şengör et al., 1985). The next idea proposed that the ancient Anatolian Triple Junction shifting from Erzincan to Karlıova occurred about 1 Ma ago, (Barka, Akyüz, Cohen, & Watchorn, 2000). The other idea proposed, the geometry and activity of the strike-slip faults that formed the boundaries between the Anatolia, African and Arabian plates was significantly different in the latest Miocene to Mid-Pliocene, the Malatya-Ovacık Fault Zone (MOFZ) (Figure 1(a)) was the former southeastern boundary of the Antaolia and its activity was ceased when the EAFZ formed (Westaway & Arger, 2001; Westaway et al., 2008). Hubert-Ferrari et al. (2009) proposed that the MOFZ is inactive during the last 3 Ma and explain that the present triple junction formed ~ 2.6 Ma ago. Supporters of opposing views propose that all strike-slip faults at the eastern part of Anatolia are actively deforming intracontinental structures (Kaymakçı, İnceöz, & Ertepınar, 2006; Koçyiğit & Beyhan, 1998). Moreover, the recent GPS measurements (Özener et al., 2010), GPS based elastic models (Aktuğ et al., 2013a, 2013b), morphochronology-based slip-rate studies (Sançar et al., 2018; Zabcı et al., 2017) and paleoseismological investigations (Sançar, Zabci, Karabacak, Yazıcı, & Akyüz, 2017; Yazıcı, Zabci, Natalin, Sançar, & Akyüz, 2018a) within the eastern part of the Anatolia strongly suggest that

these strike-slip faults are plate-boundary related structures.

The NAFZ and EAFZ intersect c. 10 km ENE of the town of Karlıova (Bingöl) and together define a V-shaped geometry opening towards the west (Figures 1 and 2). The apex point of the V-shaped structures meets the Varto Fault Zone (VFZ) and forms the KTJ, which is situated entirely within continental lithosphere (Şaroğlu & Yılmaz, 1991; Şengör, 1979; Şengör et al., 1985, 2005; Tutkun & Hancock, 1990). In the vicinity of the KTJ, the complex deformation is thought to be mainly controlled by; (a) anisotropic crustal structures of the Eastern Turkish High Plateau (ETHP; Figure 1(b)) (Şengör et al., 2008) and (b) interaction of the NAFZ and EAFZ (Şaroğlu, 1985; Şengör, 1979, 2014; Şengör et al., 1985; Tutkun & Hancock, 1990).

2.1.1. The North Anatolian Fault Zone (NAFZ)

The NAFZ is a major intracontinental strike-slip fault that initiated some 11 million years ago (Şengör et al., 2005). It has a length of c.1600 km and connects the Eastern Turkish High Plateau and the Aegean Taphrogen along a trend roughly parallel to the southern Black Sea coast (Figure 1) (Barka, 1992; Şengör, 1979; Şengör et al., 2005). In general, the NAFZ becomes wider from east to west and reaches its maximum width in the Marmara Region. Along its eastern part, around Erzincan and some 150–200 km to the west of it, fault activity is confined to a narrow zone, but further to the east it becomes wider again near Karlıova (Şengör et al., 2005).

In the Karlıova region, the NAFZ is characterized by a restraining double bend, which is defined by three fault segments (Fs1, Fs2 and Fs3 in Figure 2) between the towns of Yedisu and Karlıova (Barka & Kadinsky-Cade, 1988; Tutkun & Hancock, 1990). These three segments are considered to have partly or fully ruptured during the 17 August 1949 Elmalı Earthquake (M_s 6.9) (Ambraseys & Jackson, 1998; Barka & Kadinsky-Cade, 1988). Two further destructive earthquakes occurred in 1966, one about 40 km east of the KTJ (Ambraseys & Zatopek, 1968) and another one along the Fs1, Ilıpınar Segment (Barka & Kadinsky-Cade, 1988; Tutkun & Hancock, 1990). Although the Fs2 and Fs3 ruptured during the 1949 event, and that there is no evidence of surface faulting during the 1966 earthquake along Fs1, the Ilıpınar Segment. A single paleoseismological study across the Ilıpınar Segment did not provide any information for the last two events but instead proposes 2000 years of inter-event timing between older events (Sançar & Akyüz, 2014). This significantly longer inter-event time for the Ilıpınar Segment compared to other sections of the NAFZ to the west (e.g. Hartleb, Dolan, Akyuz, & Yerli, 2003; Kondo, Özaksoy, & Yıldirim, 2010;

Meghraoui et al., 2012; Pantosti et al., 2008) suggests that deformation in the eastern NAFZ is distributed non-homogeneously. This non-homogeneous behavior may be due to the (a) the release of energy through small and frequent earthquakes, such as the 2005 Karlıova earthquakes (Emre, Özalp, Yildirim, Özaksoy, & Doğan, 2005), and/or (b) the distribution of total strain between the main deformation zone and secondary faults (Sançar & Akyüz, 2014). The geologic slip-rate study, which claims that the main branch of the NAFZ only takes up to 55–75% (Zabcı et al., 2015a) of the total rate of about 20 mm/yr (Cavalié & Jónsson, 2014; Walters, Parsons, & Wright, 2014) and the rest of the deformation is taken up by secondary faults.

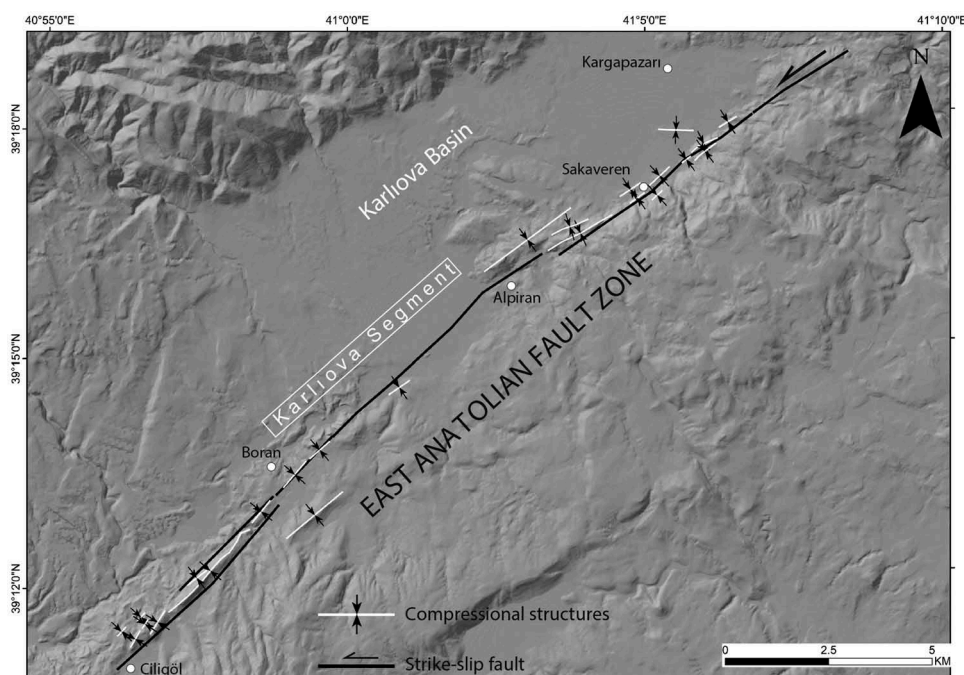### 2.1.2. The East Anatolian Fault Zone (EAFZ)

The EAFZ extends from the KTJ in the northeast to Kahramanmaraş in the southwest (Figure 1) (e.g. Allen, 1969; Barka & Kadinsky-Cade, 1988; Dewey, Hempton, Kidd, Şaroğlu, & Şengör, 1986). Some studies suggest that the EAFZ extends further to the southwest, having a length of 560 km on land, (McKenzie, 1976) and links up with the Dead Sea Fault Zone and the Cyprus Arc at the Amik Triple Junction (Duman & Emre, 2013; Perinçek & Çemen, 1990). The EAFZ is confined within a narrow deformation zone between Karlıova and Çelikhan, but gets wider farther to the southwest separating into a northern and southern strand (Duman & Emre, 2013).

The northeastern segment of the EAFZ is referred to as the Karlıova Segment (Figures 2 and 3) and is characterized by many offset features, pressure ridges, linear depressions and hot springs. The length of N55°E striking fault segment is about 25 km and extending from the KTJ to Göynük and limiting the Karlıova Basin to the SE (Figure 3). It has a relatively simple, straight geometry northeast of Sakaveren. Further to the southwest, it has a restraining step-over northeast of Alpiran and a slight restraining bend west of Alpiran, which are morphologically well marked with compressional structures (Figure 3). The Karlıova Segment gains its straight geometry again up to the village of Boran, where c. 3 km-long parallel faults occur with compressional structures in between (Figure 3). Compressional structures not only exist in between parallel fault strands and along restraining step-overs or restraining beds, but also elsewhere along the Karlıova segment, striking subparallel to the overall strike of the EAFZ. Although the southwestern neighboring segment ruptured on 22 May 1971 (M 6.8), the Karlıova segment remain un-ruptured since 1866 (Nalbant, McCloskey, Steacy, & Barka, 2002).

2.1.3. The Varto Fault Zone (VFZ)

The VFZ extends from the KTJ for about 30 km to the ESE along a widely-distributed deformation zone with a maximum width of 12 km (Sançar et al., 2015) (Figure 2). The interpretation of the structures in the VFZ is controversially discussed and several models have been proposed to explain the mechanical behavior and/or initiation of the VFZ: (a) as the eastern continuation of the NAF (Gürboğa, 2016; Ketin, 1969, 1976). (b) as a separate fault system (Sançar et al., 2015; Şaroğlu, 1988; Şengör, 1979; Şengör & Canıtez, 1982; Şengör


Figure 3. The geometry of the East Anatolian Fault Zone (EAFZ) limiting the Karlıova Basin along its southeastern margin.

et al., 1985) within an ESE striking highly convergent strain zone (Şengör, 1979; Şengör et al., 1985). (c) forming as a zipper (suture) due to the counterclockwise rotation of the EAFZ (Barka & Gülen, 1988). (d) as a result of the migrating Karlıova Triple Junction (Barka et al., 2000; Hubert-Ferrari et al., 2009; Westaway & Arger, 2001). (e) the whole zone developed as a result of distributed continental transpression (Sançar et al., 2015), or (f) The VFZ formed by at least four sub-parallel segments and fault kinematics indicate a range of shortening and extensional regimes (Karaoğlu et al., 2017).

2.1.4. Tectonic structures between the NAFZ and EAFZ in the Karlıova wedge

The Karlıova wedge is characterized as an internally deforming body at the easternmost part of Anatolian *Scholle*. The topography within the wedge is due to active tectonics resulting from westward extrusion along the NAFZ and the EAFZ (Sançar, 2014; Sançar, Zabcı, & Akyüz, 2011b). There are two major tectonic structures within the Karlıova wedge, the Bahçeköy and the Toklular Faults, which are curvilinear in map view (Emre, Duman, Olgun, Özalp, & Elmacı, 2012; Herece & Akay, 2003) (Figure 2). These faults have been defined as normal faults and their western
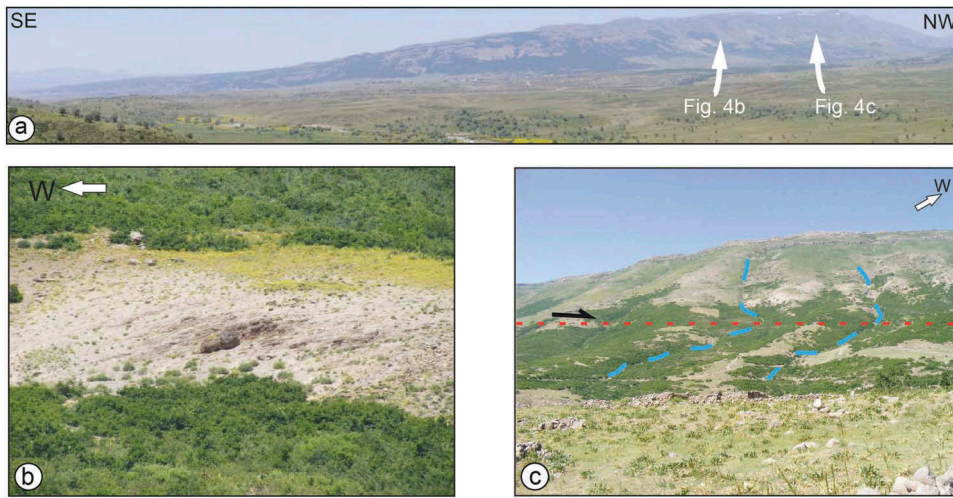
Figure 4. (a) View towards the SW of the Toklular cuesta. The slope direction of the escarpment that bounds the cuesta is towards the east, which is opposite to the west-dipping lithologies shown in (b). The systematic river offset in (c) along the western part of the escarpment of the Toklular cuesta reflects dextral oblique normal fault slip along the westernmost part of the fault before the fault changes its strike towards southeast.
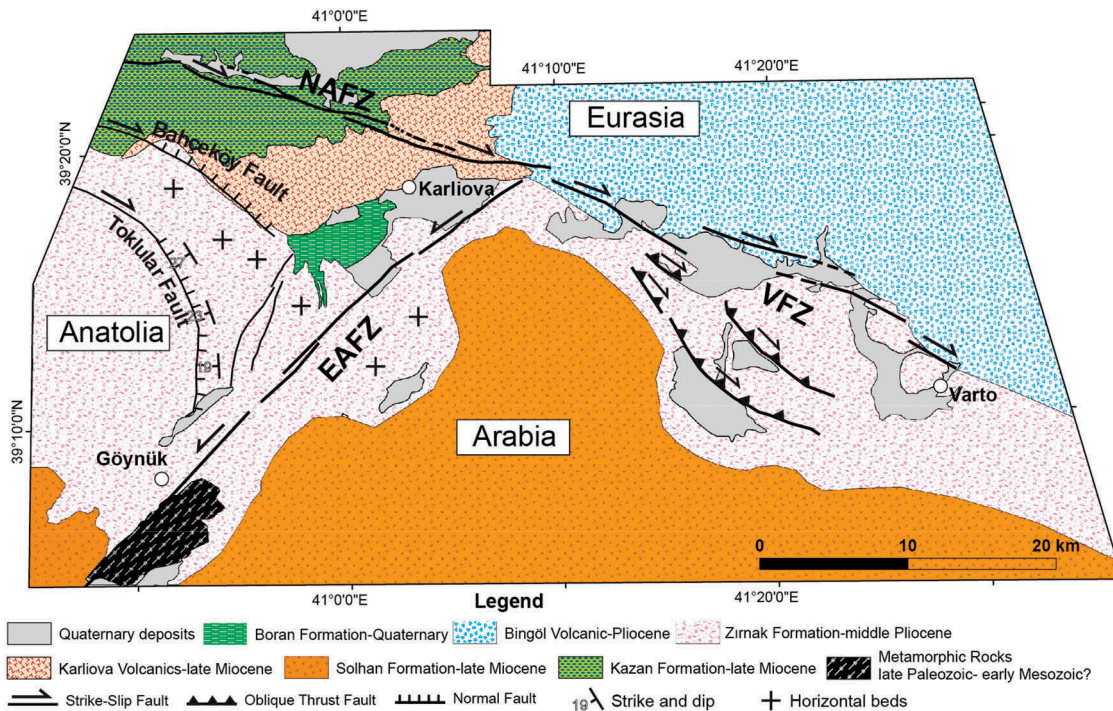
Figure 5. Geological map of the Karlıova region (modified from Şaroğlu, 1985).

continuation represented by dextral strike-slip fault (Emre et al., 2012, 2005; Herece, 2008; Hubert-Ferrari et al., 2009). The along-strike changes going from west to east, from strike-slip to normal fault, resulted in formation of cuestas, the landscapes that have a moderate slope at one side and are bordered by escarpments on the other side (Fairbridge, 1968) (Figure 4(a)). The strike-slip deformation is especially well marked along the western parts of the Bahçeköy Fault, where two streams are deflected by about 1.5 km (see white lines indicating the courses of these streams in Figure 2), but deflected river streams have also been observed along the Toklukar cuesta (Figure 4(c)). The Bahçeköy cuesta forms the boundary between Karlıova Volcanics and Zırnak Formation, whereas the Toklular cuesta formed within in Zırnak Formation. The fault-controlled steep slopes face to the east, whereas the bedding dips in the opposite direction at both cuestas (Figures 4(b) and 5). Other structures within the Karlıova wedge closer to the EAFZ consist mostly of sinistral strike-slip faults (Figure 2), which cut Holocene cover deposits and Quaternary volcanics in the Karlıova basin (Şaroğlu, 1985).

The geometry and activity of the NW-striking dextral faults and NE-striking sinistral faults within the eastern part of the Anatolian *Scholle* are the basis of the previous ideas about deformation of it (Şengör, 1979; Şengör et al., 1985; Westaway & Arger, 2001). However, the secondary faulting around the KTJ and the VFZ have been used to explain the deformation around the KTJ and put forward some regional result (Barka & Gülen, 1988). Furthermore, the strong relationship has been established between the non-homogeneous behavior of eastern part of the NAFZ and the secondary faults (Sançar et al., 2015; Zabcı et al., 2015a). In this regard, the region close to KTJ has a key spatial position to understand how deformation initiate and develop between the main fault zones and evaluate the proposed ideas about not only around the KTJ but also eastern part of the 'Ova' province.

2.1.5. The geology of the Karlıova Triple Junction and surrounding region

An overview of the geology (Figure 5) show that all tectonics structures between the NAFZ and EAFZ are active in the Plio-Quaternary in the Karlıova region. The basement consists of late Paleozoic to early Mesozoic (?) metasedimentary rocks of the Bitlis massif. An ophiolitic mélange of the Oligocene Kazan Formation overlies the basement, but the nature of the contact is not known, as it is not exposed (Şaroğlu, 1985; Şaroğlu & Yılmaz, 1991). The middle to late Miocene Solhan Formation is exposed south of the VFZ and southwest of the EAFZ, and is made up of about 1000 m-thick volcanic and volcanoclastic deposits (Şaroğlu & Yılmaz, 1991), whereas the late Miocene Karlıova volcanics include

intercalated terrestrial siliciclastics (Şaroğlu, 1985). The middle Pliocene Zırnak Formation has a transitional contact with the Karlıova volcanics and consists of pyroclastics with intercalated fluvial sandstones, lacustrine marls and limestones (Şaroğlu & Yılmaz, 1991). A 2500 m-thick sequence of Pliocene pyroclastics and lavas is referred to as the Bingöl volcanics after the Bingöl Caldera and partly covers the older units. The Quaternary Boran formation is locally exposed in the Karlıova Basin, mostly at the edge of rivers that flow into the basin. This 100 m-thick unit nonconformably overlies the Zırnak formation. The youngest Holocene (?) alluvial fan and fluvial deposits are found all over the Karlıova Basin and along the large rivers (Şaroğlu, 1985; Şaroğlu & Yılmaz, 1991).

## 3. Prandtl cell model, the karliova triple junction and the Karlıova Triple Junction wedge

The original Prandtl cell model (Prandtl, 1924) (Figure 6(a)) was subsequently modified, by using different material and boundary conditions (parallel and wedge shape boundaries) (Hartmann, 1928; Nadai, 1950; Varnes, 1962).

In the first wedge shape models(Nadai, 1950), the plates were not parallel and designed having two different conditions in which (a) the compressed material moves to a certain direction (passive case), or (b) the material flows with its own weight (active case). Slip lines are concave toward the material's movement direction in passive conditions, whereas they have a convex-shape toward the same direction in active cases (Figure 6(b) and (c)). A similar wedge model, in which the squeezed material moves to the open end of the wedge, was proposed by Varnes (1962) (Figure 6(d) and (e)) as the material was moving to the apex point of the wedge in (Nadai, 1950)'s version (Figure 6(b) and (c)). In both modified models, the slip lines form as exponential curves and only strike-slip deformation accumulated on them(Nadai, 1950; Varnes, 1962).

The wedge-shaped body (the Karlıova wedge) to the west of the KTJ that is bounded by the NAFZ in the north-northeast and the EAFZ in the southeast has geometric similarities with the passive cell models of Nadai (1950) (Figure 6(b)) and Varnes (1962), (Figure 6 (d)). However, the sense of motion along the boundary faults in the Nadai (1950) model (Figure 6(b)) does not fit the slip sense of the NAFZ and EAFZ. The westward extrusion of the Anatolian *Scholle* (Şengör et al., 1985) that is also well supported by GPS studies (e.g. McClusky et al., 2000; Reilinger et al., 2000, 2006) strongly favours the Varnes (1962)'s passive modified Prandtl cell model that the material moves to the open end of the wedge (Figure 6(d)).

In this comparison, another important parameter is the angle between the compressing plates. In the
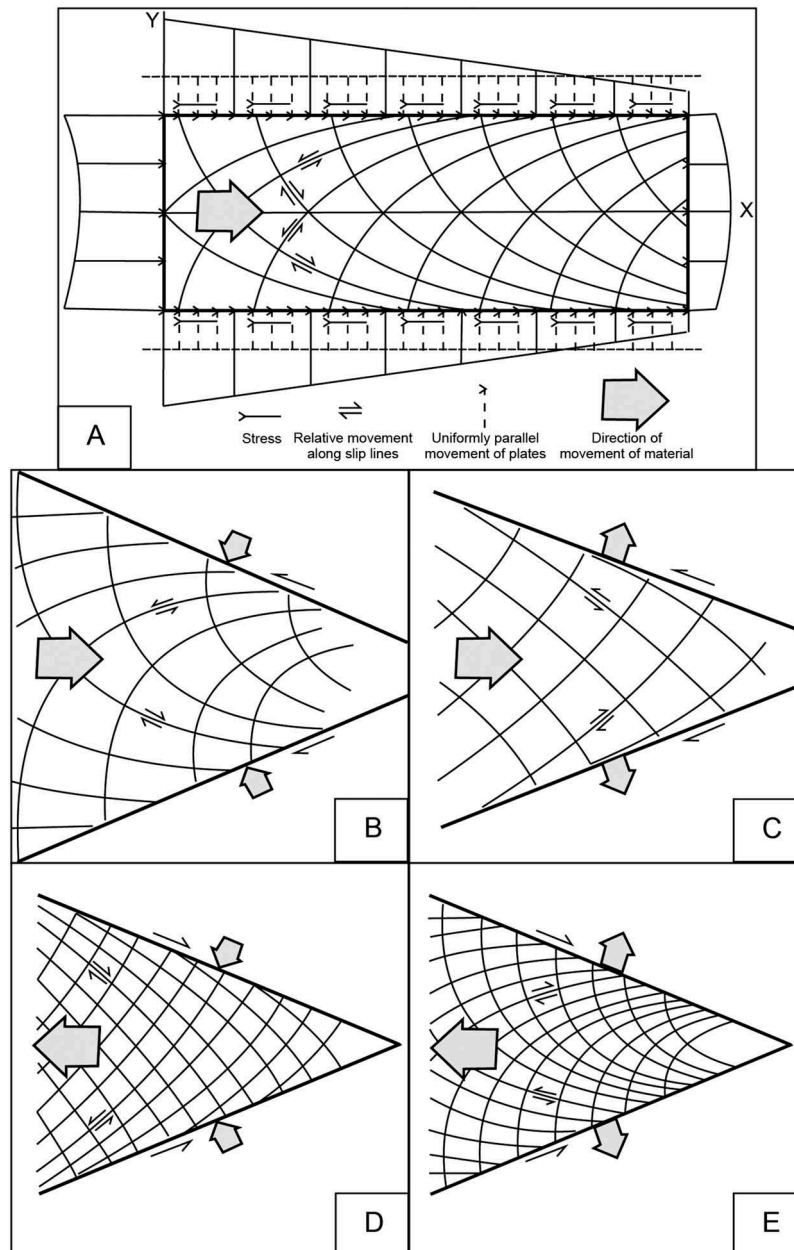
Figure 6. (a) The original Prandtl cell model (modified from Kanizay, 1962). (b) and (c) show the passive and active cases of Nadai (1950)' model, respectively (Cummings, 1976), whereas (d) shows the passive and (e) is the active settings of Varnes (1962)'s model.

original models, this angle is 48° in Nadai (1950), whereas it is 38° in Varnes (1962). We measure the angle between the NAFZ and EAFZ to be 52°- 58° in the Karlıova wedge (Figure 7) that is wider than both of the model settings. As the slip lines become more cycloid in geometry with the increasing angle, the curved geometries of Bahçeköy and Toklular faults also fit well. However, in these ideal models, all slip lines within the material inside the wedge only deform horizontally (strike-slip), where the deformation along the Bahçeköy and Toklular faults change from strike-slip to normal sense of motion as their geometry turns from linear to curvilinear to the east (Figures 2 and 7).

The comparison between the passive Prandtl cell models and structural pattern within the Karlıova

wedge clearly shows that Varnes (1962) model can explain the overall geometries of strike-slip faults, but not the vertical motions along the Bahçeköy and Toklular faults observed in nature.

4. Analogue models

4.1. Materials and experimental set-up

The internal deformation of the wedge between the NAFZ and EAFZ (between the blue vertical line and KTJ in Figure 1), has been explained with an active Prandtl cell model by Şengör (1979) and Şengör et al. (1985). However, none of the original or modified Prandtl cell models is directly analogues to the
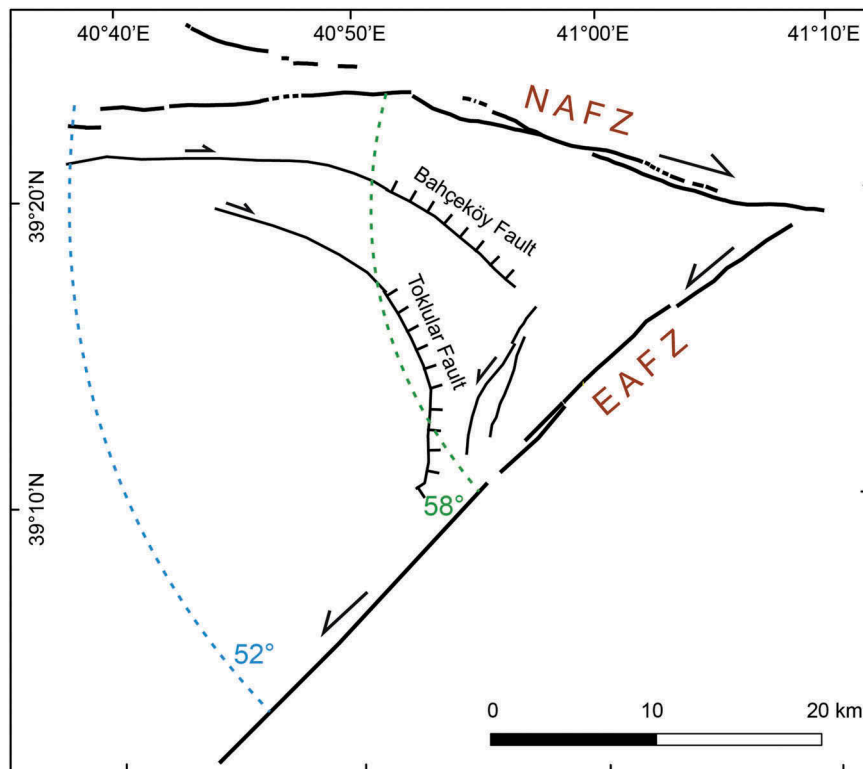
Figure 7. V-shape fault configuration defined by the North Anatolian Fault Zone (NAFZ) and East Anatolian Fault Zone (EAFZ). The angle between the strike of the two shear zones is c. 52° to 58°.

observed structures in nature, which are defined by both strike-slip and vertical motion, within the Karlıova wedge. If one considers only the strike of secondary faults within the Karlıova wedge, the modified passive V-shaped Prandtl cell model of Varnes (1962), shown in Figure 6(d), fits best the observed structures in nature. However, this model only predicts pure strike-slip motion along the slip lines and hence does not show the along strike change in fault motion of the curvilinear, secondary faults in the

Karlıova wedge, which change from strike-slip dominated to normal dip-slip dominated.

We performed a series of crustal-scale analogue experiments in order to understand the style and evolution of the Plio-Quaternary secondary faults in the KTJ region. The experimental set-up includes three basal rigid plates consisting of 1 mm thick cardboards that represent the Eurasian and Arabian Plates and the Anatolian *Scholle* (Figure 8). The rigid plate representing the Arabian Plate extends below the Eurasian Plate. In all experiments, Eurasia remains
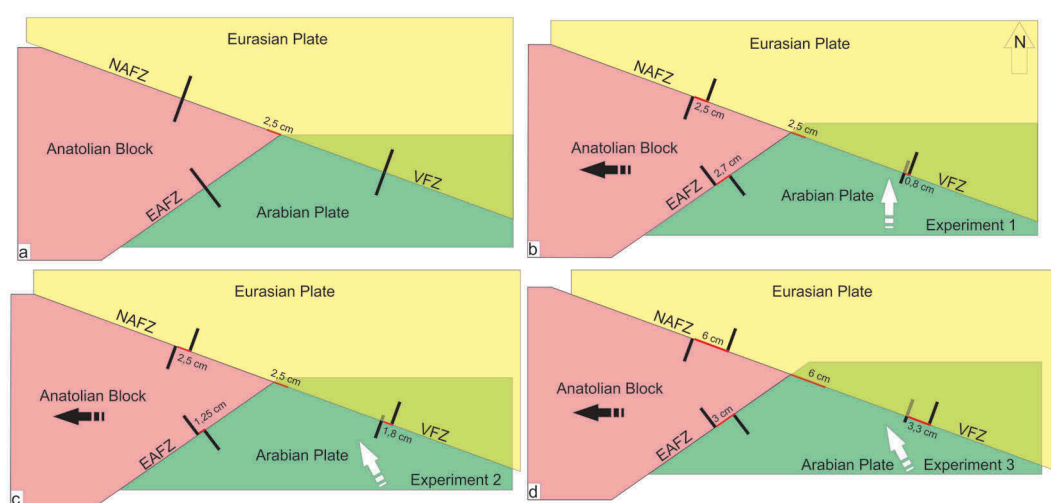
Figure 8. Schematic overview of experimental set-up used for modeling the KTJ. (a) Initial setup of all experiments. Final stages of Experiments 1, 2, 3 are shown in b, c, and d respectively. Experiments 1 and 2 uses brittle sand only, whereas experiment 3 has an additional viscous silicone layer underlying the sand.

fixed and Arabia and Anatolia move in different directions using geared motor drives. Here we represent the results of three experiments with initial model dimensions of 100 × 50 cm. In all three experiments, the relative movement between the plates organized as not to result in any gap between them. Considering the age of the NAFZ and EAFZ, although there is no age determination the VFZ, we assume that they have already been formed in Plio-Quaternary and their orientation, sense of motion and velocity of NAFZ and EAFZ are known. Furthermore, not only previous studies (Sançar, 2014; Sançar et al., 2011b; Zabcı et al., 2015a) but also the geology of the Karlıova region (Figure 5) show that the tectonic structures between the NAFZ and EAFZ in the vicinity of the KTJ have already been formed and active during the Plio-Quaternary. In order to understand causal relationship between the main fault zones (the NAFZ and EAFZ) and tectonic structures of the Karlıova region, we organize the initial orientation of the plate boundaries (basement faults) in accord with the Plio-Quaternary geometry of the triple junction components (Figure 8 (a)): The boundary between the Eurasian Plate and the Anatolian *Scholle* (future NAFZ) is oriented N70°W, as is the boundary between the Eurasian Plate and the Arabian Plate (future VFZ). The limit between the Arabian Plate and the Anatolian *Scholle* (future EAFZ) is oriented N55°E. The lateral boundaries of the model are unconfined.

In Experiment 1, that aims to test high convergent zone scenario of the VFZ (Şengör, 1979; Şengör et al., 1985), Arabia is pushed to the north underneath fixed Eurasia, whereas Anatolia is pulled at the same time to the west. The experiment ends after 2.5 cm dextral relative displacement between Eurasian and Anatolia along the NAFZ, which results in 2.7 cm of sinistral relative displacement along the EAFZ (Figure 8(b)). In Experiment 2, to test transpressional VFZ scenario, Arabia is pushed underneath fixed Eurasia towards the northwest, which is parallel to today's GPS velocity field, while Anatolia is pulled to the west. A relative movement of 2.5 cm dextral relative offset along the NAFZ results in 1.25 cm sinistral relative displacement along the EAFZ, whereas the northwest movement of Arabia causes a 1.8 cm dextral relative offset along the VFZ (Figure 8(c)). The set-up of Experiment 3 is similar to the second one, except for the magnitude of relative motions along the plate boundaries, which is 6 cm dextral for the

NAFZ, 3 cm sinistral for the EAFZ and 3.3 cm dextral along the VFZ (Figure 8(d)).

In experiments 1 and 2 we use brittle materials only with the model consisting of a 3-cm-thick layered sand cake (1.5 cm quartz and 1.5 cm corundum sand). Experiment 3 is a brittle-viscous model, consisting of a 0.75 cm thick basal viscous layer (Polydimethylsiloxane – PDMS, SGM36) overlain by a total of 3 cm of quartz and corundum sand. The quartz sand ranges in grain size between 80 and 200 μm, and has a density of 1520 kg/m³ (Klinkmüller, Schreurs, Rosenau, & Kemnitz, 2016), whereas the brown corundum sand has a grain size between 88 and 125 μm, and a density of 1890 kg/m3 (Table 1) (Panien, Schreurs, & Pfiffner, 2006). The granular materials are used to simulate the brittle upper crust. They show elastic frictional-plastic behavior with a phase of strain-hardening preceding failure at peak strength, followed by a transitional phase of strain softening (Klinkmüller et al., 2016; Lohrmann, Kukowski, Adam, & Oncken, 2003; Panien et al., 2006). Quartz and corundum sands have low cohesion and their angles of internal friction at peak strength are 35.5° and 37° (Table 1), respectively, quite similar to values determined experimentally on upper crustal rocks (Byerlee, 1978). The viscous PDMS, which is used to simulate lower crustal rocks has a density of 0.965 kgcm-3 and an average value of c. 2.8×10^4 Pa s for the viscosity in the Newtonian flow regime (Rudolf et al., 2016). In each experiment, we constructed a 5 × 5 cm surface grid by sprinkling blue colored quartz sand on top to monitor deformation in top views.
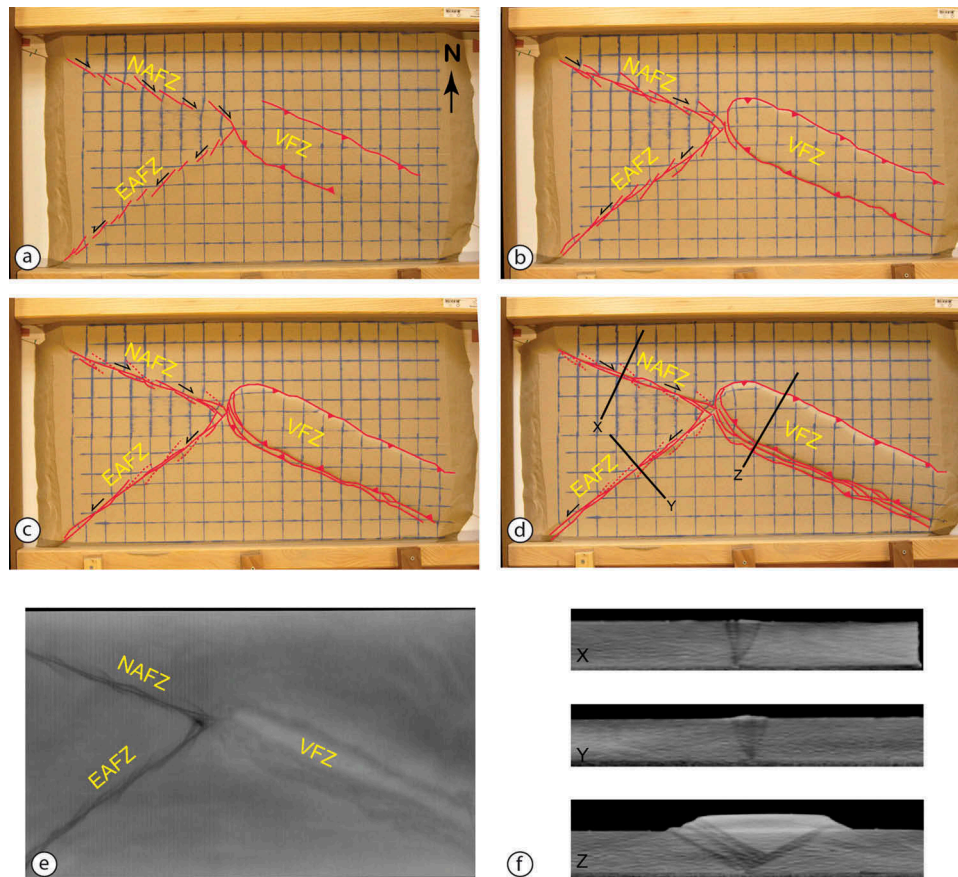
4.2. Experiment-1

During the early stages of Experiment 1, Riedel shears form along the NAFZ and EAFZ (Figure 9(a)) (See S1 for un-interpreted images). These Riedel shears (R-shears) are left stepping dextral faults along the NAFZ and right-stepping sinistral faults along the EAFZ. The en-echelon faults have a surface strike of c. 10–20° with respect to the orientation of the underlying basement fault and partly overlap creating push-up zones. A pop-up structure bounded by thrust faults forms east of the triple junction in the VFZ domain parallel to the underlying velocity discontinuity, with one of the R-shears of the NAFZ linking up laterally with a thrust fault near the triple junction point (Figure 9(a)).

Table 1. Material properties and grain characteristics.

Sand	Density kg m⁻³	C at Ø_peak (Pa)	Ø_peak (°)	Ø_stable (°)	Grain Size μm	Grain Shape	Composition
Quartz	1520	21 + 18	35.5	31.2	80–200	Angular	99% SiO₂
Corrundum	1890	39 + 10	37	32.2	88–125	Angular	95%Al₂O₃

C = cohesion; Ø_peak = angle of peak friction; Ø_stable = angle of stable-dynamic friction

Figure 9. Fault geometry in Experiment 1. (a-d) Fault evolution in map view. Red lines: R-shears and R_L-shears; Red stippled lines: inactive fault segments. (e). Horizontal X-ray CT section at c. 1.5 cm above base of model. (f) three vertical X-ray CT sections through model. For location of sections see Figure 9(d).

With increasing deformation R-shears along the NAFZ and the EAFZ coalesce in two different ways: (1) as closely adjacent R shears propagate along strike their surface strike decreases in the overlap region and they merge with an adjacent R shear, (2) with the help of R_L-shears (Schreurs, 2003) that form in the overlap region between two adjacent R-shears. The R_L-shears have the same sense of displacement as R-shears, but lower surface strikes (Figure 9(c,d)). The coalescence of R-shears leaves inactive fault segments behind (stippled red lines in Figure 9(c,d)), as the main displacement progressively localizes along the through-going fault (the principal displacement zone, PDZ), which strikes subparallel to the underlying basement fault. The relief between the PDZ and the inactive fault segments becomes more pronounced with progressive deformation (Figure 9(c, d)). Meanwhile, further thrusts propagating in-sequence to the SSW form along the southern part of the VFZ domain, causing a pronounced pop-up structure with noticeable vertical relief (Figure 9(c,d)). The horizontal section at depth (c. 1 cm above the base of the model) illustrates both the through-going PDZ along the NAFZ and EAFZ, and the faults segments that have become inactive and strike at an angle to the PDZ (Figure 9(e)). The vertical sections in Figure 9(f) show flower structures consisting of steep to vertical faults along the

NAFZ and the EAFZ, and the pop-up structure defining the VFZ domain (Movie S1).

4.3. Experiment-2

In Experiment 2 left-stepping en-echelon R-shears form initially along the NAFZ striking at angles of c. 10–20° to the basement fault, except near the triple junction where the R shear strikes at a higher angle of c. 25° (Figure 10(a)) (See S2 for un-interpreted images). At this stage no faulting is yet visible along the EAFZ, and only a diffuse zone of deformation (clockwise rotation of the surface grid) is visible east of the triple junction in the VFZ domain (Figure 10(a)).

With increasing deformation en echelon R shears form also along the EAFZ striking at angles of c. 15–20° to the basement fault. At the same time R_L shears connect initial R-shears along the NAFZ forming a PDZ (Figure 10(b)). East of the triple junction one of the R-shears along the NAFZ propagates SE-ward and merges with an emerging thrust fault in the VFZ domain (Figure 10(b)).

With progressive deformation, the oblique shortening between Arabia and Anatolia results in a partitioning of fault motion in the VFZ domain, with thrust dominated faulting along its southern margin and more
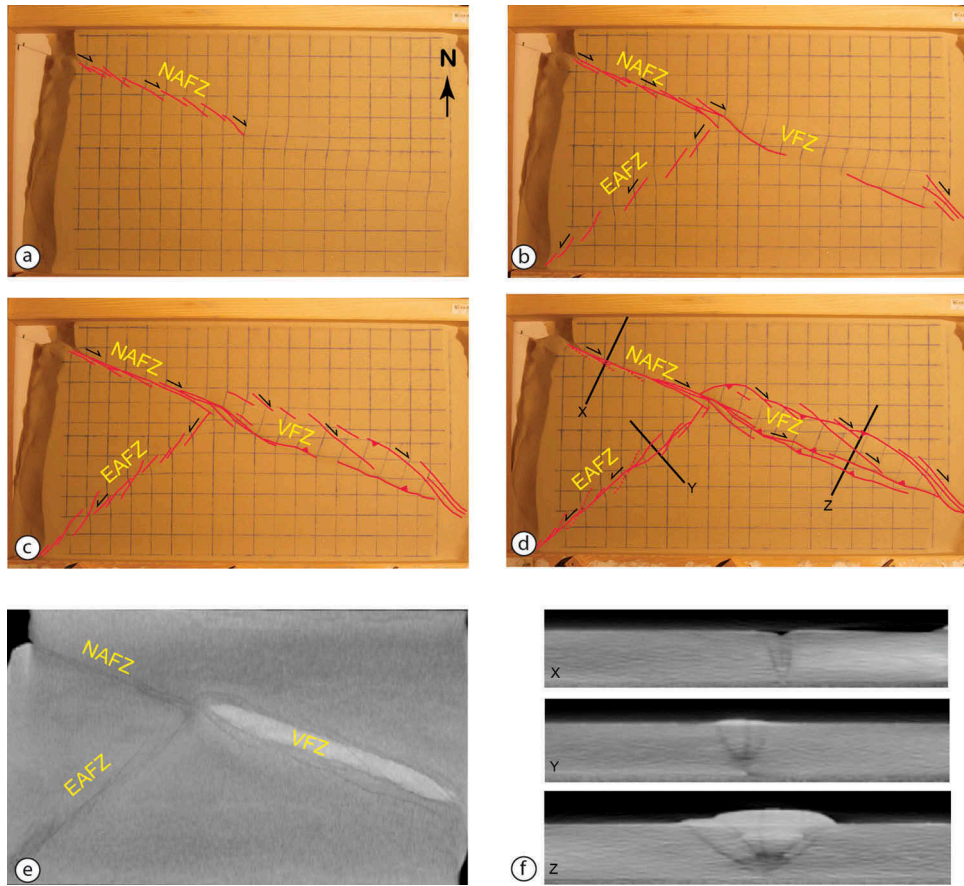
Figure 10. Fault geometry in Experiment 2. (a-d) Fault evolution in map view. Red lines: R-shears and R_L-shears; Red stippled lines: inactive fault segments. (e). Horizontal X-ray CT section at c. 1.5 cm above base of model. (f) three vertical X-ray CT sections through model. For location of sections see Figure 10(d).

dextral strike-slip dominated faulting along its northern margin (Figure 10(c)). In the final stage, a transpressive pop-up structure has formed along the VFZ consisting of downward verging dextral oblique-slip thrust faults and dextral strike-slip faults that are mostly confined within the pop-up (Figure 10(d)). There is considerable clockwise rotation of the material within the pop-up structure. With some delay, progressive deformation also results in the formation of a PDZ along the EAFZ, with faults outside the PDZ becoming largely inactive. The uplift between the PDZ and the inactive fault segments is higher along the EAFZ than along the NAFZ
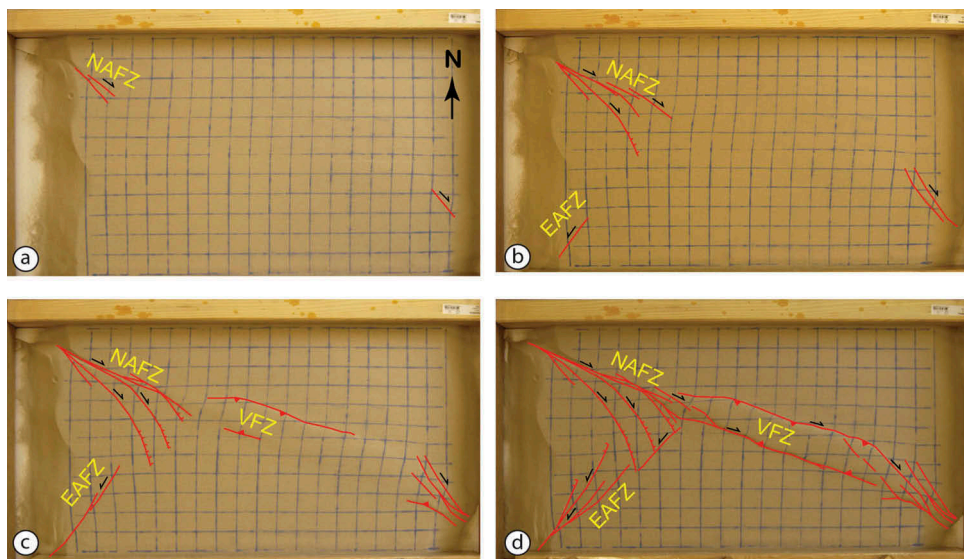
Figure 11. Fault evolution in map view of experiment 3. Red lines: R-shears and R_L-shears; Red stippled lines: inactive fault segments.

(Figure 10(d)). The horizontal X-ray CT section in Figure 10(e) shows the well-developed PDZ along the NAFZ and the less pronounced PDZ along the EAFZ. In the VFZ domain, the lighter part represents uplifted corundum sand (which has a higher material density and hence a different grey shade in X-ray CT image than the less dense quartz sand) occupying the central region of the transpressive pop-up structure (Figure 10(e)). Fault traces within the light region strike at an angle to the overall strike of the thrust belt and merge with the thrust faults (Figure 10(e)). Figure 10(f) illustrates the geometry of flower structures through the NAFZ and EAFZ (section X and Y, respectively), and the downward converging thrust faults of the transpressive pop-up structure with vertical strike-slip faults merging with the thrust fault at depth (section Z) (Movie S2).

4.4. Experiment-3

As in the previous Experiment 2, en echelon R-shears develop first along the NAFZ (Figure 11(a)) whereas faults along the EAFZ form later (Figure 11(b)) (See S3 for un-interpreted images). In the VFZ domain, dextral strike-slip faults form near the lateral boundary of the model (Figure 11(a,b)). With increasing deformation the R shears along the NAFZ propagate towards the SE and acquire a curvilinear geometry in surface view (Figure 11(b)). With progressive deformation the curvilinear nature of the faults becomes more pronounced as they propagate to the SSE away from the boundary fault underling the NAFZ into the wedge region defined by the northern and southeastern boundaries of the Anatolian *Scholle*. The curvilinear faults have a strike-slip component near the NAFZ, but along strike to the southeast this strike-slip component diminishes and is gradually taken over by a small dip-slip component (see normal fault signature in Figure 11(b)). At the same time, a PDZ forms along the NAFZ as R_L-shears in between overlapping R shears and link up with them (Figure 11(c)). En echelon R shears now also form along the EAFZ (Figure 11(b,c)) and thrusting and associated bulging in the VFZ domain (Figure 11(c)) illustrates the formation of an incipient pop-up structure with the downward converging thrusts obtaining a dextral strike-slip component with progressive deformation (Figure 11(d)). Material within this transpressive pop-up structure undergoes a clockwise rotation (Figure 11(c,d)). Faults of the PDZ along the NAFZ link up with thrusts that form in the VFZ domain (Figure 11(d)). At the end of the experiment, some of the R shears along the EAFZ are deflected towards the north and also obtain a curvilinear shape in map view, and also acquire a slight dip-slip component of movement at their tips. No through-going PDZ has yet formed along the EAFZ, and the strike-slip component of movement near the triple junction is limited (Movie S3).

4.5. Experiments results

Our experiments have the same boundary conditions except for the orientation of the movement directions of the plates (identical in Experiment 2 and 3, but different in Experiment 1) and/or in mechanical layering (brittle only in experiments 1 and 2, and brittle-viscous in Experiment 3).

In Experiment 1, the NAFZ and the EAFZ each have a well-developed PDZ, whereas the structures along the VFZ are distributed in a wide zone consisting of a pop-up structure confined by pure thrust faults (Figure 9). Although Experiment 2 also results in the formation of a PDZ along the NAFZ and the EAFZ, in contrast to Experiment 1, the vertical relief along overlapping fault segments along the EAFZ is more pronounced due to the NW directed movement of Arabia with respect to Anatolia (which was N directed in experiment 1). Cross-sections through the PDZ of the EAFZ show a clear flower structure (Figure 10(f), section Y) with a steep central strike-slip fault (part of the PDZ) and less steeply dipping subparallel faults merging at depth with the central steep fault and having a reverse component of slip. As in Experiment 1, a wide deformation zone forms along the VFZ in experiment 2 (Figure 10). However, the VFZ forms as a dextral transpressive pop-up structure due to the oblique movement of Arabia with respect to Eurasia. Cross-sections through the VFZ clearly show the pure thrust faults confining the pop-up structure in experiment 1 (Figure 9(f), section Z), and the transpressive pop-up structure of experiment 2 (Figure 10(f), section Z), with subvertical strike-slip faults confined between the downward-verging thrusts.

In Experiment 1, the NAFZ and the EAFZ form coevally (Figure 9). In contrast, in experiment 2 and 3 (Figures 10 & 11) faulting along the EAFZ on the brittle layer forms at later stages than in Experiment 1. This is related to the relative displacements along the NAFZ and EAFZ basement faults which is nearly equal in experiment 1 (2.5 cm and 2.7 cm, respectively), and which is twice as large for the NAFZ (compared to EAFZ) in experiments 2 and 3. In all experiments a PDZ forms along the NAFZ and EAFZ, except in experiment 3 where it is not fully developed along the EAFZ.

Only in the brittle-viscous experiment 3 we do have the development of secondary faults in the wedge between the NAFZ and EAFZ (Figure 11). These faults start out as R shears that form above the boundary faults separating Eurasia from Anatolia and Anatolia from Arabia. As these faults propagate along strike in the wedge region, they acquire a curvilinear shape in map view. Slip is dominated by strike-slip movement along the initial linear segment of the faults, but the dip-slip component becomes more and more pronounced along strike as the fault propagates and curves. As relative displacement is more important

along the Eurasian/Anatolian boundary in experiment 3, these curvilinear faults emanate first from the NAFZ. At late stages of experiment 3, curvilinear faults also propagate into the wedge away from the EAFZ. As in experiment 2, which has the same NW directed relative movement of the Arabian plate, a transpressive pop-up structures forms east of the triple point in the VFZ domain.

As the only difference between experiment 2 and 3 is the mechanical stratigraphy of the model, we propose that the westward flow of viscous material in the wedge between the NAFZ and EAFZ exerts an important influence on the fault pattern forming in the overlying brittle sand layers. We infer that the sideways movement of viscous material at the base causes the curvilinear shape of the faults in the wedge and the dip-slip component as faults propagate along strike.

The fault pattern shown in Figure 3, shows strong similarities to experiment 3. The Bahçeköy and Toklular faults are almost identical in orientation and character to the secondary faults forming in the analogue model. The natural faults are dominated by strike-slip movements in their western part, but then acquire a curvilinear geometry going eastward where have a more southeasterly strike and where relative movement is dominated by a normal dip-slip component.

Experiment 3 presents not only the almost identical fault geometry as in nature, but it also successfully provides ideal physical conditions (the angle between the V-shaped PDZs, the magnitude of relative motion, a lower viscous layer) to have the curvilinear faults with normal sense of motion at their ends. Therefore, we also make an important contribution to the previous compressive Prandtl cell model of Varnes (1962) with the introduction of slip-lines not only for pure strike-slip faults, but also with a normal dip-slip component of deformation.

5. Discussions

The Karlıova Triple Junction is one of the peculiar structure in the Eastern Mediterranean region. Explaining of how deformation initiate and develop around the KTJ provide key clue(s) to understand the deformation that related to interaction of the NAFZ and EAFZ in eastern part of the Anatolian *Scholle*, where active structures interpreted as products of the Prandtl cell model (Şengör, 1979; Şengör et al., 1985).

To understand the faulting mechanisim, we performed three analouge experiments. Experiment 1 and 2 do not match perfectly to the mapped structures in the KTJ and its vicinity.

In Experiment 1, the NAFZ and the EAFZ characterized by a well-developed PDZ and there is no deformation between them. The northward motion of the Arabian Plate, which cause to high convergent strain

along the VFZ, create only the pop-up structure with noticeable vertical relief confined by pure thrust faults along the VFZ, although 0,8 cm strike-slip offset occurred (Figure 9). Şengör (1979) and Şengör et al. (1985) propose that eastern component of the KTJ, the Varto Fault Zone, is a high convergent zone which have similar structures with the Experiment 1 result. However, nature of the VFZ is not pure thrust fault as described in recent studies (Gürboğa, 2016; Hubert-Ferrari et al., 2009; Karaoğlu et al., 2017; Sançar et al., 2015)

In Experiment 2, structures were observed differently from Experiment 1; (a) the vertical relief along the EAFZ, which we match the compressional structures along the it (Figure 4) (b) and the transpressive pop-up structures along the VFZ that is reflect to the nature of the transpressional VFZ (Sançar et al., 2015)

The secondary faults that between the NAFZ and EAFZ, only develop in the Experiment 3 (Figure 11). In accordance with what is seen in the nature (Bahçeli and Toklular faults) (Figure 2), the sense of motion change from strike-slip to oblique normal and then to pure normal slip going from west to the east in Experiment 3 (Figure 11). These curvilinear faults initiate from the NAFZ at beginning of the Experiment 3, propagate into the wedge and terminate around the EAFZ. Development of these faults support the idea, which depend upon paleoseismological (Sançar & Akyüz, 2014) and slip-rate studies (Zabcı et al., 2015a), non-homogeneous deformation in the easternmost part of the NAFZ, close the KTJ, is due to distribution of total strain between the main deformation zone and secondary faults. Furthermore, to explain the initiation and development of these faults by using their geometry and sense of motion passive wedge-shaped Prandtl cell model of Varnes (1962) is more appropriate to explain the overall, regional fault pattern than the previously proposed active Prandtl cell model by (Şengör, 1979; Şengör et al., 1985). Once again, we emphasize that those slip-lines described in Varnes (1962) not only for pure strike-slip faults, but also with a normal dip-slip component of deformation. We suggest that Varnes (1962) passive Prandtl cell model with a normal dip-slip component along slip lines is more appropriate model not only around the KTJ but also for the eastern part of the Anatolian *Scholle*.

The fault pattern along the VFZ in Experiment 3 is characterized by a transpressional pop-up structure east of the KTJ with significant uplift (Figure 11(a-d)), which is suggested to happen with a rate of 0.35 mm/yr (Sançar et al., 2015) and is similar to results from other transpressional experiments (Schreurs, 2003; Schreurs & Colletta, 1998).

The structural elements of the VFZ in nature (or generally all of them within its vicinity) are considered to be part of either a PDZ or a transpressional splay zone (Gürboğa, 2016), or products of a poly-phased tectonic evolution (Karaoğlu et al., 2017). We do not observe any

transtensional deformation during any stages of Experiment 3. However, we need to consider that local extensional structures may simultaneously form in compressional settings. Therefore, these extensional faults may not indicate any regional transtensional or extensional deformation east of the KTJ, but can represent synchronous (or diachronous) structures of a long-lived compressional deformation. In this case, the normal fault of Karaoğlu et al. (2017) can be an extensional structure that is formed within the extensional part of Sançar et al. (2015)'s regional strain ellipse and is then rotated for about 20°-25° in a clockwise sense. In conclusion, we suggest that all structures of the VFZ in Experiment 3 or as they are mapped in nature (Sançar et al., 2015) form part of a distributed transpressional system, which experiences continuous oblique shortening since the formation of the KTJ.

In a more general sense, Experiment 3 also provides important information on the discussion about the stationary or migrating models of the KTJ and deformational structures within eastern part of the 'Ova' province. In the stationary model, the Anatolian *Scholle* is suggested to wedge out from the 'jaws of the converging plates of Eurasian and Arabian', while the KTJ is held *in situ* and the gap (or hole) formed within the wedge is closed with complex faulting and intense vulcanicity (Şengör, 1979; Şengör et al., 1985). We show that the faulting mechanisms resulted from Experiment 3 is the responsible one that help to close gap.

The idea of migrating triple junction is proposed by multiple studies: (a) one suggesting the triple junction jumped from the Erzincan region to the Karlıova (migration from west to east) after the initiation of the EAF (Westaway & Arger, 2001; Westaway et al., 2008). (b) The zipper VFZ due to the anticlockwise rotation of the EAFZ and east – west-trending thrust structures formed within the wedge, (Barka & Gülen, 1988). (c) the locally slight decrease in the InSar velocity field is also interpreted to be the result of westward migration of the triple junction in time (Cavalié & Jónsson, 2014), However, neither the Malatya-Ovacık Fault is an inactive fault (Aktuğ et al., 2013a, 2013b; Arpat & Şaroğlu, 1975; Kaymakçı et al., 2006; Özener et al., 2010; Sançar et al., 2018; Yazıcı et al., 2018a; Zabcı et al., 2017, 2015b; Zabcı, Sançar, Tikhomirov, Vockenhuber, & Ivy-Ochs, 2014), nor the E-W striking thrust faults of the zipper model can be observed to the west of the KTJ (Herece, 2008; Hubert-Ferrari et al., 2009; Sançar, Akyüz, & Zabcı, 2011a; Sançar et al., 2011b) and/or at the end of Experiment 3. The elastic block models suggest horizontal slip rates between 1.2 ± 0.3 mm/a and 1.6 ± 0.3 mm/a (Aktuğ et al., 2013a) or 1.8 ± 0.1 and 1.2 ± 0.1 mm/a (Aktuğ et al., 2013b) for, the Ovacık Fault and the Malatya Fault in the NE and SE of the MOFZ, respectively whereas morphochronolgy based slip-rate studies suggest 2.7 mm/a (Zabcı et al., 2017)

and 1.2 mm/a (Sançar et al., 2018) respectively. Paleoseismological studies estimate 1600 ± 515 yr., (Yazıcı et al., 2018a) and 2275 ± 605 (Sançar et al., 2017) average earthquake recurrence interval on the same faults. Considering that if the slip-rate of the faults change between time 0.1–10 mm/a. and earthquake recurrence change between 10^2–10^4 yr., these faults are tectonically related to the plate boundaries or formed in diffuse plate boundaries (Scholz 2002), we propose that the strike-slip faults within the eastern part of the Anatolia are plate boundary related intraplate active structures. The Experiment 3 reveal that intraplate deformation of eastern part of the Anatolia is similar to the passive Prandtl cell model.

6. Conclusions

In conclusion, the pattern of Plio-Quaternary faulting around the KTJ, particularly to the west of the triple junction, has been the most important effect in the tectonic evolution of the region. The strong similarities of faulting, in terms of their geometries and sense of motions between the Karlıova wedge and eastern part of Anatolia, are results of the interaction between the NAFZ and EAFZ. Our results, as summarized below, contribute to the future studies not only for this interesting part of the Eastern Mediterranean region but also for other continental settings that are formed by V-shaped strike-slip faults.

1. We claim that not only our field observations on secondary faults (Bahçeli and Toklular), but also our results in Experiment 3 strongly support passive Prandtl cell model with normal sense of motion along the slip lines and are components of the faulting mechanism since Plio-Quaternary at the western part of the KTJ.

2. Considering that, there are strong similarities between strike-slip faults within the Karlıova wedge and the eastern part of the Anatolian *Scholle* where deformation characterized by NW-striking dextral and NE-striking sinistral strike-slip faults, we propose that the passive Prandtl cell model is appropriate to explain the internal deformation of eastern part of the Anatolia.

3. Non-homogenous distribution of deformation, which exhibits itself by the irregular earthquake behaviour with significantly longer recurrence interval (Sançar & Akyüz, 2014) and the relatively lower geologic slip-rates along the main fault branch (Zabcı et al., 2015a) at the eastern part of the NAFZ, is result of the accumulated strain on the secondary faults since Plio-Quaternary.

4. Experiment 3 supports a long-lived distributed transpressive setting (Sançar et al., 2015) to the east of the KTJ, rather than previous models about the VFZ such as; high convergent zone(Şengör,

1979; Şengör et al., 1985), zipper zone due to CCW rotation of the EAFZ (Barka & Gülen, 1988), as a transpressional termination to the NAFZ (Gürboğa, 2016), and a range of shortening and extensional regimes (Karaoğlu et al., 2017).

Acknowledgments

Disclosure statement

Funding

ORCID

H. Serdar Akyüz http://orcid.org/0000-0001-9485-2017

References

Aktuğ, B., Dikmen, U., Dogru, A., & Ozener, H. (2013a). Seismicity and strain accumulation around karliova triple junction (Turkey). *Journal of Geodynamics*, *67*, 21–29.

Aktuğ, B., Parmaksız, E., Kurt, M., Lenk, O., Kılıçoğlu, A., Gürdal, M. A., & Özdemir, S. (2013b). Deformation of central anatolia: GPS implications. *Journal of Geodynamics*, *67*(Supplement C), 78–96.

Akyuz, H. S., Altunel, E., Karabacak, V., & Yalciner, C. C. (2006). Historical earthquake activity of the northern part of the dead sea fault zone, southern Turkey. *Tectonophysics*, *426* (3–4), 281–293.

Allen, C. R. (1969). *Active faulting in northern Turkey* (Vol. 1577, pp. 32). California: Division of Geological Sciences, California Institute of Technology. ContributionNo. 1577.

Ambraseys, N. N., & Jackson, J. A. (1998). Faulting associated with historical and recent earthquakes in the eastern mediterranean region. *Geophysical Journal International*, *133*(2), 390–406.

Ambraseys, N. N., & Zatopek, A. (1968). The varto ustukran (Anatolia) earthquake of 19 august 1966 summary of a field report. *Bulletin of the Seismological Society of America*, *58*(1), 47–102.

Arpat, E., & Şaroğlu, F. (1975). Türkiye'deki bazı önemli genç tektonik olaylar (on some important young tectonic events in Turkey). *Bulletin of the Geological Society of Turkey*, *18*, 29–41.

Avagyan, A., Sosson, M., Karakhanian, A., Philip, H., Rebai, S., Rolland, Y., … Davtyan, V. (2010). Recent tectonic stress evolution in the lesser caucasus and adjacent regions. *Geological Society, London, Special Publications*, *340*(1), 393.

Barka, A., Akyüz, H. S., Cohen, H. A., & Watchorn, F. (2000). Tectonic evolution of the niksar and tasova-erbaa pull-apart basins, North anatolian fault zone: Their significance for the motion of the anatolian block. *Tectonophysics*, *322* (3–4), 243–264.

Barka, A. A. (1992). The North Anatolian fault zone. *Annales Tectonicae*, *6*(Suppl.), 164–195.

Barka, A. A., & Gülen, L. (1988). *New constraints on age and total offset of the North anatolian fault zone: Implications for tectonics of the Eastern mediterranean region, 1987 Melin Tokay Symposium* (pp. 39–65). Ankara: Spec. Publ. Middle-east Technical University.

Barka, A. A., & Kadinsky-Cade, K. (1988). Strike-slip fault geometry in Turkey and its influence on earthquake activity. *Tectonics*, *7*(3), 663–684.

Bozkurt, E. (2001). Neotectonics of Turkey; a synthesis. *Geodinamica Acta*, *14*(1–3), 3–30.

Byerlee, J. (1978). Friction of rocks. *Pure and Applied Geophysics*, *116*(4–5), 615–626.

Cavalié, O., & Jónsson, S. (2014). Block-like plate movements in eastern anatolia observed by InSAR. *Geophysical Research Letters*, *41*(1), 26–31.

Cronin, V. S. (1992). Types and kinematic stability of triple junctions. *Tectonophysics*, *207*(3–4), 287–301.

Cummings, D. (1976). Theory of plasticity applied to faulting, Mojave Desert, southern California. *Geological Society of America Bulletin*, *87*(5), 720–724.

Dewey, J. F., Hempton, M. R., Kidd, W. S. F., Şaroğlu, F., & Şengör, A. M. C. (1986). Shortening of continental lithosphere: The neotectonics of Eastern anatolia – A young collision zone. In M. P. Coward & A. C. Ries (eds.), *Collision Tectonics* (Vol. 19, pp. 3–36). London: Geological Society Special Publication.

Duman, T. Y., & Emre, Ö. (2013). The east anatolian fault: Geometry, segmentation and jog characteristics. In A. H. F. Robertson, O. Parlak, & U. C. Ünlügenç̧ (eds.), *Geological development of anatolia and the Easternmost mediterranean region* (Vol. 372, pp. 495–529). London: Geological Society, Special Publications.

Emre, Ö., Duman, T. Y., Olgun, Ş., Özalp, S., & Elmacı, H. (2012). *1:250.000 Ölçekli Türkiye Diri Fay Haritası Serisi, Erzurum (NJ37-4) Paftası, Seri No:48*. Ankara-Türkiye: Maden Tetkik ve Arama Genel Müdürlüğü.

Emre, Ö., Özalp, S., Yildirim, C., Özaksoy, V., & Doğan, A. (2005). *12 ve 14 Mart Karlıova Depremleri'nin Değerlendirilmesi*. Ankara, Turkey: Maden Tetkik ve Arama Genel Müdürlüğü.

Faccenna, C., Becker, T. W., Jolivet, L., & Keskin, M. (2013). Mantle convection in the middle east: reconciling afar upwelling, arabia indentation and aegean trench rollback. *Arabia Indentation and Aegean Trench Rollback: Earth and Planetary Science Letters*, *375*, 254-269. doi:10.1016/j.epsl.2013.05.043

Fairbridge, R. W. (1968). *The encyclopedia of geomorphology*. New York: Reinhold Book Corporation.

Gordon, R. G. (1998). THE PLATE TECTONIC APPROXIMATION: Plate nonrigidity, diffuse plate boundaries, and global plate reconstructions. *Annual Review of Earth and Planetary Sciences*, *26*(1), 615–642.

Gürboğa, Ş. (2016). The termination of the North anatolian fault system (NAFS) in Eastern Turkey. *International Geology Review*, *58*(12), 1557–1567.

Hall, J., Aksu, A. E., Elitez, I., Yaltırak, C., & Çifçi, G. (2014). The fethiye–burdur fault zone: A component of upper plate extension of the subduction transform edge propagator fault linking Hellenic and Cyprus Arcs, Eastern mediterranean. *Tectonophysics*, *635*(Supplement C), 80–99.

Hartleb, R. D., Dolan, J. F., Akyuz, H. S., & Yerli, B. (2003). A 2000-year-long paleoseismologic record of earthquakes along the central North anatolian fault, from trenches at Alayurt, Turkey. *Bulletin of the Seismological Society of America*, *93*(5), 1935–1954.

Hartmann, W. (1928). *in Nadai: Das gleichgewicht lockerer Massen: Plastizitat und Erdruck, Handbuch der Physik* (Vol. 6, pp. 484–501). Berlin: Springer-Verlag.

Herece, A., & Akay, E. (2003). *Kuzey Anadolu Fay (KAF) Atlası/ Atlas of North Anatolian Fault (NAF)* (pp. 61). Ankara: Maden Tetkik ve Arama Genel Müdürlüğü, Özel Yayın, Ser. 2.

Herece, E. 2008. *Atlas of East anatolian fault*. Special Publication Series. Ankara, Turkey: General Directorate of Mineral Research and Exploration, Special Publication Series.

Higgins, M., Schoenbohm, L. M., Brocard, G., Kaymakci, N., Gosse, J. C., & Cosca, M. A. (2015). New kinematic and geochronologic evidence for the quaternary evolution of the Central Anatolian fault zone (CAFZ). *Tectonics*, *34*(10), 2118–2141.

Hubert-Ferrari, A., Armijo, R., King, G., Meyer, B., & Barka, A. A. (2002). Morphology, displacement, and slip rates along the North anatolian fault, Turkey. *Journal of Geophysical Research*, *107*(B10), 2235.

Hubert-Ferrari, A., King, G., Woerd, J. V. D., Villa, I., Altunel, E., & Armijo, R. (2009). Long-term evolution of the North anatolian fault: New constraints from its eastern termination. *Geological Society, London, Special Publications*, *311*(1), 133–154.

Ingles, J., Dauch, C., Soula, J.-C., Viallard, P., & Brusset, S. (1999). Application of the prandtl-nadai cell model to a regional scale fault intersection: The grésigne-quercy block (SW France. *Journal of Structural Geology*, *21*(4), 449–466.

Jarvis, A., Reuter, H., Nelson, A., & Guevara, E. (2008). *Hole-filled seamless SRTM data V4*. International Centre for tropical Agriculture (CIAT). http://srtm.csi.cgiar.org

Kanizay, S. P. (1962). Mohr's theory of strength and prandtl's compressed cell in relation to vertical tectonics: *USGS Professional Paper*. Vol. 414-B.

Karaoğlu, Ö., Selçuk, A. S., & Gudmundsson, A. (2017). Tectonic controls on the karliova triple junction (Turkey): Implications for tectonic inversion and the initiation of volcanism. *Tectonophysics*, *694*, 368–384.

Kaymakçı, N., İnceöz, M., & Ertepınar, P. (2006). 3D- architecture and neogene evolution of the malatya basin: Inferences for the kinematics of the malatya and Ovacik Fault Zones. *Turkish Journal of Earth Sciences*, *15*, 123–154.

Ketin, İ. (1969). Kuzey Anadolu Fayı Hakkında. *Maden Tetkik ve Arama Dergisi*, *72*, 1–27.

Ketin, İ. (1976). San Andreas ve Kuzey Anadolu Faylari arasinda bir karşılaştırma. *Türkiye Jeoloji Kurumu Bülteni*, *19*, 149–154.

Klinkmüller, M., Schreurs, G., Rosenau, M., & Kemnitz, H. (2016). Properties of granular analogue model materials: A community wide survey. *Tectonophysics*, *684*, 23–38.

Koçyiğit, A., & Beyhan, A. (1998). A new intra-continental transcurrent structure: The central Anatolian Fault Zone, Turkey. *Tectonophysics*, *284*, 317–336.

Kondo, H., Özaksoy, V., & Yıldirim, C. (2010). Slip history of the 1944 bolu-gerede earthquake rupture along the North anatolian fault system: Implications for recurrence behavior of multisegment earthquakes. *Journal of Geophysical Research*, *115*(B4), 1–16.

Kozacı, O., Dolan, J. F., & Finkel, R. C. (2009). A late holocene slip rate for the central North anatolian fault, at Tahtaköprü, Turkey, from cosmogenic 10Be geochronology: Implications for fault loading and strain release rates. *Journal of Geophysical Research: Solid Earth*, *114*(B1), 1–12.

Le Pichon, X. (1968). Sea-floor spreading and continental drift. *Journal of Geophysical Research*, *73*(12), 3661–3697.

Le Pichon, X., Chamot-Rooke, N., L., S., Noomen, R., & Veis, G. (1995). Geodetic determination of the kinematics of central greece with respect to Europe: Implications for eastern mediterranean tectonics. *Journal of Geophysical Research: Solid Earth*, *100*, 12675–12690.

Le Pichon, X., & Kreemer, C. (2010). The miocene-to-present kinematic evolution of the Eastern mediterranean and middle East and its implications for dynamics. *Annual Review of Earth and Planetary Sciences*, *38*(1), 323–351.

Lohrmann, J., Kukowski, N., Adam, J., & Oncken, O. (2003). The impact of analogue material properties on the geometry, kinematics and dynamics of convergent sand wedges. *Journal of Structural Geology*, *25*, 1691–1711.

Marques, F. O., Cobbold, P. R., & Lourenço, N. (2007). Physical models of rifting and transform faulting, due to ridge push in a wedge-shaped oceanic lithosphere. *Tectonophysics*, *443*(1–2), 37–52.

McClusky, S., Balassanian, S., Barka, A., Demir, C., Ergintav, S., Georgiev, I., ... Veis, G. (2000). Global positioning system constraints on plate kinematics and dynamics in the eastern mediterranean and caucasus. *Journal of Geophysical Research*, *105*(B3), 5695–5719.

McKenzie, D. (1972). Active tectonics of the mediterranean region. *Geophysical Journal of the Royal Astronomical Society*, *30*(2), 109–185.

McKenzie, D. (1976). The east anatolian fault: A major structure in Eastern Turkey. *Earth and Planetary Science Letters*, *29*(1), 189–193.

McKenzie, D. P., & Morgan, W. J. (1969). Evolution of triple junctions. *Nature*, *224*(5215), 125–133.

McKenzie, D. P., & Parker, R. L. (1967). The North Pacific: An example of tectonics on a sphere. *Nature*, *216*(5122), 1276–1280.

Meghraoui, M., Aksoy, M. E., Akyüz, H. S., Ferry, M., Dikbaş, A., & Altunel, E. (2012). Paleoseismology of the North Anatolian Fault at Güzelköy (Ganos segment, Turkey): Size and recurrence time of earthquake ruptures west of the sea of Marmara. *Geochemistry, Geophysics, Geosystems*, *13*, Q04005.

Morgan, W. J. (1968). Rises, trenches, great faults, and crustal blocks. *Journal of Geophysical Research*, *73*(6), 1959–1982.

Nadai, A. (1950). *Theory of fracture and flow of solids*. New York: McGraw-Hill.

Nalbant, S. S., McCloskey, J., Steacy, S., & Barka, A. A. (2002). Stress accumulation and increased seismic risk in eastern Turkey. *Earth and Planetary Science Letters*, *195*(3–4), 291–298.

Nyst, M., & Thatcher, W. (2004). New constraints on the active tectonic deformation of the Aegean. *Journal of Geophysical Research: Solid Earth*, *109*(B11), 1-23.

Özener, H., Arpat, E., Ergintav, S., Dogru, A., Cakmak, R., Turgut, B., & Dogan, U. (2010). Kinematics of the eastern part of the North Anatolian Fault Zone. *Journal of Geodynamics*, *49*(3–4), 141–150.

Panien, M., Schreurs, G., & Pfiffner, A. (2006). Mechanical behaviour of granular materials used in analogue modelling: Insights from grain characterisation, ring-shear tests and analogue experiments. *Journal of Structural Geology*, *28*, 1170–1724.

Pantosti, D., Pucci, S., Palyvos, N., Martini, P. M. D., D'Addezio, G., Collins, P. E. F., & Zabcı, C. (2008). Paleoearthquakes of the duzce fault (North Anatolian Fault Zone): Insights for large surface faulting earthquake recurrence. *Journal of Geophysical Research*, *113*, B01309–B01309.

Perinçek, D., & Çemen, İ. (1990). The structural relationship between the East anatolian and dead sea fault zones in southeastern Turkey. *Tectonophysics*, *172*, 331–340.

Philip, H., Cisternas, A., Gvishiani, A., & Gorshkov, A. (1989). The caucasus: An actual example of the initial stages of continental collision. *Tectonophysics*, *161*(1–2), 1–21.

Prandtl, L. (1924). Anwendungsbeispiele zu einem Henckyschen Satz iiber das plastische Gleichgewicht: Zeitschr. angew. *Mathematik Und Mechanik*, *3*, 401–407.

Ratschbacher, L., Merle, O., Davy, P., & Cobbold, P. (1991). Lateral extrusion in the eastern alps, part 1: Boundary conditions and experiments scaled for gravity. *Tectonics*, *10*(2), 245–256.

Reilinger, R., McClusky, S., Vernant, P., Lawrence, S., Ergintav, S., Cakmak, R., … Karam, G. (2006). GPS constraints on continental deformation in the Africa-Arabia-Eurasia continental collision zone and implications for the dynamics of plate interactions. *Journal of Geophysical Research*, *111*(B5), B05411.

Reilinger, R. E., Ergintav, S., Bürgmann, R., McClusky, S., Lenk, O., Barka, A., … Töksoz, M. N. (2000). Coseismic and postseismic fault slip for the 17 august 1999, M = 7.5, Izmit, Turkey Earthquake. *Science*, *289*(5484), 1519–1524.

Royer, J.-Y., & Gordon, R. G. (1997). The motion and boundary between the capricorn and Australian plates. *Science*, *277*(5330), 1268.

Rudolf, M., Boutelier, D., Rosenau, M., Leever, K., Schreurs, G., & Oncken, O. (2016). Rheological benchmark of silicone oils used for analog modeling of short- and long-term lithospheric deformation. *Tectonophysics*, *684*, 12–22.

Sançar, T. (2014). *Karlıova Üçlü Eklemi'nin Kuvaterner Evrimi* (Doktora). İTÜ-Avrasya Yer Bilimleri Enstitüsü. p. 239.

Sançar, T., & Akyüz, H. S. (2014). Kuzey Anadolu Fay Zonu, Ilıpınar Segmenti'nin (Karlıova, Bingöl) Paleosismolojisi. *Türkiye Jeoloji Bülteni*, *57*(2), 35–52.

Sançar, T., Akyüz, H. S., & Zabcı, C. (2011a). *Quaternary faulting mechanism around the karliova triple junction* (EGU2011-5040). Vienna: EGU, Geophysical Research Abstracts.

Sançar, T., Zabcı, C., & Akyüz, H. S. (2011b). *Morphometric analysis of secondary faults around the Karlıova Triple Junction* (EGU2011-4991). Vienna: EGU, Geophysical Research Abstracts.

Sançar, T., Zabcı, C., Akyüz, H. S., Sunal, G., & Villa, I. M. (2015). Distributed transpressive continental deformation: The Varto Fault Zone, eastern Turkey. *Tectonophysics*, *661*, 99–111.

Sançar, T., Zabci, C., Akçar, N., Karabacak, V., Yazıcı, M., Akyüz, H. S., … Vockenhuber, C. (2018). *Intraplate deformation of the anatolian scholle: Insights from morphochronolgy-based uplift and slip rates of the Malatya fault* (EGU2018-6442-3). Eastern Turkey: EGU General Assembly Vienna.

Sançar, T., Zabci, C., Karabacak, V., Yazıcı, M., & Akyüz, H. S. (2017). *Paleoseismic history of the Malatya fault (Malatya-Ovacık Fault Zone, Eastern Anatolian scholle) for the last 10 ka* (EGU2017-2948).Vienna: EGU General Assembly.

Sarıkaya, M. A., Yıldırım, C., & Çiner, A. (2015). No surface breaking on the ecemiş fault, central Turkey, since Late Pleistocene (~64.5 ka); new geomorphic and geochronologic data from cosmogenic dating of offset alluvial fans. *Tectonophysics*, *649*, 33–46.

Şaroğlu, F. (1985). Doğu Anadolu'nun Neotektonik Dönemde Jeolojik ve Yapısal Evrimi(Doktora Unpublished PhD). İstanbul Üniversitesi, p. 240.

Şaroğlu, F. (1988). *Age and offset of the North anatolian fault, 1987 melih tokay symposium* (pp. 65–79). Ankara: Spec. Publ. Middle-East Technical University.

Şaroğlu, F., & Yılmaz, Y. (1991). Geology of the karliova region: Intersection of the North anatolian and East Anatolian Transform Faults. *Bulletin Technical University Istanbul*, *44*, 475–493.

Şaroğlu, F., Emre, Ö., & Kuşçu, İ. (1992). *Türkiye Diri Fay Haritasi (Active Faut Map of Turkey)* (scale 1:2000000). one sheet. Maden Tetkik ve Arama Genel Müdürlüğü, Ankara, Turkey: Maden Tetkik ve Arama Genel Müdürlüğü.

Scholz, C. H. (2002). *The Mechanics of Earthquake and Faulting*(2nd ed., pp. 471). Cambridge University Press.

Schreurs, G. (2003). Fault development and interaction in distributed strike-slip shear zones: An experimental approach. In F. Storti, R. E. Holdsworth, & F. Salvini (eds.), *Intraplate strike-slip deformation belts* (Vol. ume 210, pp. 35–52). London: Geological Society, Special Publications.

Schreurs, G., & Colletta, B. (1998). Analogue modelling of faulting in zones of continental transpression and transtension. *Geological Society, London, Special Publications*, *135*(1), 59–79.

Searle, M. P., Chung, S.-L., & Lo, C.-H. (2010). Geological offsets and age constraints along the northern dead sea fault, Syria. *Journal of the Geological Society*, *167*, 1001–1008.

Şengör, A. M. C. (1979). The North Anatolian transform fault; its age, offset and tectonic significance. *Journal of the Geological Society of London*, *136*(Part 3), 269–282.

Şengör, A. M. C. (1980). *Türkiye Neotektoniğinin Esasları (Principles of the Neotectonism of Turkey)* (pp. 40). Ankara, Turkey: Türkiye Jeoloji Kurumu Yayını.

Şengör, A. M. C., & Canıtez, N. (1982). The North Anatolian Fault. In H. Berekhemer & K. Hsü (eds.), *Alpine mediterranean geodynamics* (Vol. 7, pp. 205–216). American Geophysical Union.

Şengör, A. M. C., Görür, N., & Şaroğlu, F. (1985). Strike slip faulting and related basin formations in zones of tectonic escape: Turkey as a case study. In K. T. Biddle & N. Christie-Blick (eds.), *Strike-slip faulting and basin formation, society of economic paleontologists and mineralogists* (pp. 227–264). Tulsa, Oklahoma: Special Publication No. 37.

Şengör, A. M. C., Tüysüz, O., İmren, C., Sakınç, M., Eyidoğan, H., Görür, N., … Rangin, C. (2005). The North Anatolıan fault: A new look. *Annual Review of Earth and Planetary Sciences*, *33*(1), 37–112.

Şengör, A. M. C., Özeren, M. S., Keskin, M., Sakínç, M., Özbakir, A. D., & Kayan, I. (2008). Eastern Turkish high plateau as a small Turkic-type orogen: Implications for post-collisional crust-forming processes in Turkic-type orogens. *Earth-Science Reviews*, *90*(1–2), 1–48.

Şengör, A. M. C., Grall, C., İmren, C., Le Pichon, X., Görür, N., Henry, P., … Siyako, M. (2014). The geometry of the North anatolian transform fault in the sea of Marmara and its temporal evolution: Implications for the development of

intracontinental transform faults. *Canadian Journal of Earth Sciences*, 51(3), 222–242.

Şengör, A. M. C. (2014). Triple Junction. In J. Harff, M. Meschede, S. Petersen, & J. Thiede (eds.), *Encyclopedia of marine geosciences* (pp. 1–13). Dordrecht: Springer Netherlands.

Shaw, B., & Jackson, J. (2010). Earthquake mechanisms and active tectonics of the hellenic subduction zone. *Geophysical Journal International*, 181(2), 966–984.

Tapponnier, P., Peltzer, G., & Armijo, R. (1986). On the mechanics of the collision between India and Asia. *Geological Society, London, Special Publications*, 19(1), 113–157.

Taylor, M., & Yin, A. (2009). Active structures of the himalayan-tibetan orogen and their relationships to earthquake distribution, contemporary strain field, and cenozoic volcanism. *Geosphere*, 5(3), 199–214.

Tutkun, S. Z., & Hancock, P. L. (1990). Tectonic landforms expressing strain at the Karliova continental triple junction (E. Turkey). *Annales Tectonicae*, 4, 182–195.

Varnes, D. J. (1962). Analysis of plastic deformation according to von mises' theory, with application to the South Silverton area, San Juan County, Colorado. *USGS Professional Paper*. Vol. 378-B.

Walters, R. J., Parsons, B., & Wright, T. J. (2014). Constraining crustal velocity fields with InSAR for Eastern Turkey: Limits to the block-like behavior of Eastern Anatolia: Journal of geophysical research. *Solid Earth*, 119(6), 5215–5234.

Wessel, P., Smith, W. H. F., Scharroo, R., Luis, J., & Wobbe, F. (2013). Generic mapping tools: Improved version released. *Eos, Transactions American Geophysical Union*, 94(45), 409–410.

Westaway, R., & Arger, J. (2001). Kinematics of the malatya-ovacik fault zone. *Geodinamica Acta*, 14(1–3), 103–131.

Westaway, R., Demir, T., & Seyrek, A. (2008). Geometry of the Turkey-Arabia and Africa-Arabia plate boundaries in the latest miocene to mid-pliocene: The role of the malatya-ovacik fault zone in eastern Turkey. *eEarth*, 3(1), 27–35.

Wilson, J. T. (1965). A new class of faults and their bearing on continental drift. *Nature*, 207(4995), 343–347.

Yazıcı, M., Zabcı, C., Sançar, T., & Natalin, B. A. (2018b). The role of intraplate strike-slip faults in shaping the surrounding morphology: The ovacik fault (eastern Turkey) as a case study. *Geomorphology*, 321, 129–145.

Yazıcı, M., Zabcı, C., Sançar, T., Sunal, G., & Natalin, B. A. (2016). *Preliminary results on the tectonic activity of the Ovacık Fault (Malatya-Ovacık Fault Zone, Turkey)*. Vienna,

Austria: Implications of the morphometric analyses, EGU General Assembly.

Yazıcı, M., Zabci, C., Natalin, B. A., Sançar, T., & Akyüz, H. S. (2018a). *Strike-slip deformation in a converging setting: Insights from the Ovacık Fault (Anatolia, Turkey)* (EGU2018-1052). Vienna: EGU General Assembly.

Yıldırım, C. (2014). Relative tectonic activity assessment of the tuz gölü fault zone; Central Anatolia, Turkey. *Tectonophysics*, 630, 183–192.

Yıldırım, C., Sarıkaya, M. A., & Çiner, A. (2016). Late pleistocene intraplate extension of the central anatolian Plateau, Turkey: Inferences from cosmogenic exposure dating of alluvial fan, landslide, and moraine surfaces along the Ecemiş Fault Zone. *Tectonics*, 35(6), 1446–1464.

Yin, A. (2010). Cenozoic tectonic evolution of Asia: A preliminary synthesis. *Tectonophysics*, 488(1–4), 293–325.

Yin, A., & Taylor, M. H. (2011). Mechanics of V-shaped conjugate strike-slip faults and the corresponding continuum mode of continental deformation. *Geological Society of America Bulletin*, 123(9–10), 1798–1821.

Zabcı, C., Sançar, T., Akyüz, H. S., & Kıyak, N. G. (2015a). Spatial slip behavior of large strike-slip fault belts: Implications for the holocene slip rates of the eastern termination of the North anatolian Fault, Turkey. *Journal of Geophysical Research: Solid Earth*, 120(12), 8591–8609.

Zabcı, C., Sançar, T., Tikhomirov, D., S., I. -O., Vockenhuber, C., Friedrich, A. M., Yazıcı, M., Akçar, N. (2017). *Cosmogenic 36 Cl Geochronology of Offset Terraces Along The Ovacık Fault (Malatya-Ovacık Fault Zone, Eastern Turkey): Implications for the Intra-plate Deformation of the Anatolian Scholle, The International Conference on Astronomy & Geophysics in Mongolia*, Ulaanbaatar-Mongolia.

Zabcı, C., Sançar, T., Tikhomirov, D., Ivy-Ochs, S., Vockenhuber, C., & Akçar, N. (2015b). *The preliminary slip rates of the Ovacık Fault (Turkey) for the last 16 ka: Implications for the intraplate deformation of the Anatolian 'scholle', XIX INQUA* (T01074). Nagoya Japan.

Zabcı, C., Sançar, T., Tikhomirov, D., Vockenhuber, C., & Ivy-Ochs, S. 2014. *Preliminary geologic slip rates of the Ovacık Segment (Malatya-Ovacık Fault, Turkey) for the last 15 ka: Insights from cosmogenic 36Cl dating of offset fluvial surfaces. Proceedings EGU*, Wien.

Özeren, M. S., & Holt, W. E. (2010). The dynamics of the Eastern Mediterranean and Eastern Turkey. *Geophysical journal international*, 183(3), 1165-1184. doi:10.1111/j.1365-246X.2010.04819.x